ELECTRICAL RESISTANCE OF DILUTE Mg (Mn) ALLOYS BELOW 1° K

by

Gilles Gaudet

Submitted in partial fulfillment of
the requirements for the degree
of Master of Science.

Department of Physics,
Faculty of Pure and Applied Science,
The University of Ottawa,
Ottawa, Canada,
1960.

ABSTRACT

The electrical resistance of magnesium-manganese solid solutions has been measured in the liquid helium range and below 1° K. The results are given in this thesis with details of the cryostat for adiabatic demagnetization and of the galvanometer amplifier used to measure the resistance.

Many authors have reported the existence of a minimum in the resistance of Mg (Mn) alloys at low temperatures. Some of them have conjectured that a resistance maximum might exist below this minimum. However they did not observe this maximum because their specimens did not contain enough Mn in solid solution to produce a maximum in the range of temperatures of the observations.

Techniques developped in this laboratory have made it possible to keep more Mn in solid solution. A resistance maximum was observed in these specimens and the preliminary results were published recently by Gaudet, Hedgcock, Lamarche and Wallingford (1960).

The measurements reported here were taken on Mg specimens containing from 0.07 to 0.4 atomic % Mn in solid solution. The temperature of the maximum (T_{max}) increases with the concentration of Mn from about 1° K to 5° K. The resistance decreased rapidly below the maximum without any clear evidence

of levelling off near 0.2^{0} K.

The magnetoresistance of a few specimens was measured in fields up to 5 kOe at liquid helium temperatures. It did not obey Kohler's rule but decreased markedly on cooling and even became negative around T_{max}.

A brief survey of the recent theories on the resistance anomalies of dilute magnetic alloys is also given. It attempts to bring out the important features of these theories and some problems that remain unsolved. In particular it became evident that it would be useless to attempt a detailed comparison between any of these theories and the experimental results reported here.

ACKNOWLEDGMENTS

I wish to express my gratitude to Dr. Gilles Lamarche who has introduced me to the techniques of low temperature physics and has helped me to continue and complete this research project.

I wish also th thank the professors and students of the Department for many interesting discussions and useful suggestions. In particular I want to thank Errol Wallingford who has been most helpful on many occasions.

Financial assistance was received from the National Research Council through the research grant A-723 and it is gratefully acknowledged.

TABLE OF CONTENTS

		Page
ABSTRACT		III
ACKNOWLEDGMENTS		V
LIST OF FIGURES		X
LIST OF TABLES		XII
CHAPTER 1		
1.1	Introduction	1
1.2	Resistivity of Normal Dilute Alloys	3
1.2.1	Mathiessen's Rule	3
1.2.2	Resistivity due to Thermal Vibrations	4
1.2.3	Impurity Resistivity	6
1.2.4	Detailed Calculation of Current.	7
1.3	Resistivity of Dilute Magnetic Alloys .	12
1.3.1	Large Deviations from Mathiessen's Rule	12
1.3.2	Resistivity due to Thermal Vibrations	16
1.3.3	Anomalous Impurity Resistivity .	17
1.3.4	Mechanisms Proposed to Explain the Anomalous Impurity Resistivity of Dilute Magnetic Alloys	18

	Page
(a) Particular Electronic Structure ...	18
(b) Magnetic Interactions between Impurities	20
(c) Spin-Disorder Theory	26
1.3.5 Summary of the Theories on the Resistance Anomalies of Dilute Magnetic Alloys	27
1.4 Magnetoresistance of Normal Dilute Alloys	30
1.4.1 Kohler's Rule	31
1.4.2 Further Remarks on Magnetoresistance	32
1.5 Magnetoresistance of Dilute Magnetic Alloys	33
1.5.1 Deviations from Kohler's Rule	
1.5.2 Polarization of Spins by an External Magnetic Field	34
1.5.3 Theories on the Negative Magneto-resistance	35
CHAPTER 2	
2.1 Introduction	37
2.2 Cryostat	37
2.2.1 Liquid Helium Temperatures	39
2.2.2 Cooling below 1^{0} K	41

		Page
2.3	Mounting of the Resistance Specimen and Paramagnetic Salt	42
2.4	Paramagnetic Salts and the Salt Container	45
2.5	Measurement of Temperature below 1° K .	46
	2.5.1 Thermal Equilibrium	46
	2.5.2 Susceptibility Bridge	47
	2.5.3 Magnetic Susceptibility of the Salt Sample	52
	2.5.4 Calibration of Susceptibility Bridge	55
	2.5.5 Carbon Resistor as Thermometers Below 1° K	57
2.6	Measurement of Electrical Resistance ..	59
	2.6.1 Method	59
	2.6.2 Galvanometer Amplifier	61
	2.6.3 Remarks on the Choice of Galvanometers for Amplifier	65
	2.6.4 Details of the Galvanometer Amplifier	66
	2.6.5 Varying Capacities, Thermal Noise and Vibrations	66
	2.6.6 Precision of Resistance Measurements	68

Page

2.7 Measurements of Magnetoresistance 69

2.7.1 Method and Mounting 69

2.7.2 Electromagnet 69

2.8 Precision of Measurements 71

2.9 Preparation of Mg (Mn) Specimens 73

CHAPTER 3

3.1 Previous Measurements on Mg (Mn) Alloys 78

3.2 Results of Resistance and Magnetoresistance Measurements on Mg (Mn) Alloys 80

3.3 Conclusions 89

BIBLIOGRAPHY 91

LIST OF FIGURES

Page

Figure 1 - Four types of behaviour of the electrical resistance of dilute magnetic alloys 14

2 - (a) Photograph of the cryostat 38

2 (b) Details of magnet, dewars and high vacuum chamber 38

3 - Mounting of the resistance specimen and paramagnetic salt 43

4 - Magnetic susceptibility bridge 48

5 - Modified Julius suspension for the ballistic galvanometer 50

6 - Drawing of susceptibility coils 51

7 - Current source of specimen 60

8 - Circuit of galvanometer amplifier ... 62

9 - Simplified wiring of the amplifier .. 62

10 - Linearlity of the galvanometer amplifier 64

11 - Optical system of the galvanometer amplifier 67

12 - Photograph of galvanometer amplifier 67

13 - Variation of H across the pole faces . 70

Page

Figure 14 - Mounting of specimen for magneto-resistance 70

15 - Estimate of atomic % Mn in Mg versus the normalized ratio $R_{4.2}/(R_{273}-R_{4.2})$ 77

16 - Relative electrical resistance versus temperature of two dilute Mg (Mn) alloys 82

17 - Relative electrical resistance versus temperature of the two most concentrated Mg (Mn) solid solutions 83

18 - Temperature of the resistance maximum of Mg (Mn) alloys versus $R_{4.2}/(R_{273}-R_{4.2})$ 85

19 - Magnetoresistance plots of a dilute Mg (Mn) alloy 87

20 - Magnetoresistance of two specimens of Mg (Mn) at temperatures near the resistance maximum 88

LIST OF TABLES

		Page
Table 1 -	Theories on the resistance anomalies of dilute magnetic alloys	28
2 -	Preparation of Specimens	75
3 -	Tabulation of resistance and magneto-resistance measurements on a few Mg (Mn) alloys	81

CHAPTER 1

1.1 Introduction

The discovery of an anomalous phenomenon often stimulates the experimental and the theoretical work in a given field of physics. In 1933 de Haas and van den Berg have observed a minimum in the electrical resistance of a gold specimen at low temperatures. They expected only a monotonic decrease in the resistance with decreasing temperature. This anomalous minimum has later been observed in the resistance of many other metals.

During the last decade it has been shown that very small quantities of transition element impurities are responsible for the anomalous minimum. Also it has been observed that higher concentrations of these paramagnetic impurities (e.g. 0.1 atomic % of Mn in Cu) often cause a resistance maximum below the minimum. In this thesis we are particularly interested in this anomalous resistance maximum.

Other anomalies have also been observed in the properties of dilute magnetic alloys; for example anomalies have been observed in the magnetoresistance, magnetic susceptibility, nuclear magnetic resonance, electron spin resonance, specific heat, thermal conductivity, Hall coefficient, etc.

These observations and the work of theoretical physicists have given us a better knowledge not only of dilute magnetic alloys, but of all metals.

The present work is an experimental study of the electrical resistance of Mg (Mn) alloys at temperatures below 1° K. This research was started with the hope of establishing whether or not a maximum occurred in the resistance of magnetic alloys with divalent parent metals. Such a behavior had been observed only in dilute magnetic alloys with monovalent parent metals; e.g. Cu (Mn), Ag (Mn), Au (Cr).

Such a maximum has eventually been observed in the resistance of a Mg (Mn) alloy at 1.2° K and was subsequently observed at higher temperatures with more concentrated Mg (Mn) alloys.

We have also attempted to establish whether or not the resistance maximum of Mg (Mn) alloys is similar in nature and origin to the maxima previously observed in dilute magnetic alloys with monovalent parent metals. A negative magnetoresistance is always observed around the temperature of a resistance maximum. To complete our investigation, the magnetoresistance of Mg (Mn) alloys has therefore been studied at liquid helium temperatures.

In this first chapter we try to summarize the normal behavior and the anomalous behavior of both the electrical resistance and the magnetoresistance of dilute alloys. In each case we first present the experimental facts and then we give a brief summary of the theories proposed to explain these facts.

The apparatus and the experimental methods are described in the second chapter along with the accuracy of measurements.

Our observations and conclusions are presented in the third chapter.

1.2 Resistivity of Normal Dilute Alloys

1.2.1 Mathiessen's rule

The dilute alloys are normally expected to obey Mathiessen's rule. That is, the increase in resistivity ρ_B due to a small concentration of foreign atoms in solid solution is independent of temperature. If the total resistivity is denoted by $\rho(T)$,

$$\rho(T) = \rho_T(T) + \rho_B \qquad (1)$$

where $\rho_T(T)$ is the resistivity due to thermal vibrations and ρ_B the constant resistivity due to impurities.

Mathiessen's rule requires that the impurity resistivity be the same at all temperatures. However it also implies that the thermal resistivity ρ_T of the alloy and pure metal follow the same law and that the thermal and impurity resistivity are independent and simply add up. Such a behavior is fairly well understood. Normally an impurity introduces in the lattice a perturbation that is independent of temperature. This is one of the reasons why the impurity resistivity is usually constant. On the other hand the thermal component of the resistivity depends on the lattice vibrations. The few impurities present in a dilute alloy do not affect appreciably the lattice vibrations. Therefore the thermal resistivity of the pure metal and of the alloy are approximately equal. Finally the total resistivity depends on the total amount of scattering. The thermal scattering and impurity scattering are relatively weak processes independent of each other and their effects usually simply add up.

1.2.2 Resistivity due to Thermal Vibrations

When an electron is scattered by the lattice vibrating at frequency ν_1 it exchanges a quantum of energy $h\nu_1$ with it. These exchanges of energy are essentially inelastic. However in this thesis the term inelastic scattering will be

used exclusively to describe events where the electronic structure of an impurity is changed in a collision with a conduction electron.

The Debye model may be used to describe the thermal vibrations of a metal. It is then possible to calculate the relaxation time τ and the resistivity as a function of temperature. If the interactions between the electrons and the lattice are simplified, we may obtain the Bloch-Grüneisen formula

$$\rho = \frac{KT^5}{M\Theta^6} \int_0^{\Theta/T} \frac{z^5 \, dz}{(e^z-1)(1-e^{-z})} \qquad (2)$$

where M is the atomic weight and K is a constant characteristic of the metal and its volume. The thermal resistivity is zero near 0° K and it increases monotonically with temperature. For $T/\Theta = 0.1$, $\rho \approx 124 \frac{KT^5}{M\Theta^6}$. For $T = 0.1\ \Theta$, the thermal resistivity is about 5×10^{-3} its value at $T = \Theta$. For magnesium, $\Theta_D \approx 290^\circ$ K so that at 30° K the resistivity due to thermal vibrations is about 5×10^{-3} its value at room temperature.

If the thermal resistivity of a dilute alloy is not the same as for the pure metal there will be deviations from Matthiessen's law. Small deviations from Matthiessen's rule are actually observed in the resistivity of most dilute alloys.

they may be caused by changes in the lattice characteristic frequency θ_D due to the presence of foreign atoms.

1.2.3 Impurity Resistivity

As previously mentioned, the impurity resistivity of normal alloys does not vary with the temperature. The scattering of conduction electrons by impurities is usually considered elastic scattering, i.e. only the direction of motion of the electrons is changed and not their energy. The impurities cause scattering because their field is different from the field of the solvent atoms. It is the difference between these two fields that is regarded as the cause of the impurity scattering; i.e. only deviations from periodic potentials cause scattering.

If the foreign atom has the same valency as the atom it substitutes, the impurity resistivity ρ_i will usually be small. However when the valency of the foreign atom differs from the one of the pure metal by Z, the impurity resistivity is usually much larger and proportional to Z^2 (Norbury's rule). The Coulomb forces seem to be mainly responsible for the scattering. Norbury's rule is explained by assuming that all valence electrons go into the conduction band and that Rutherford's Z^2 law of scattering holds. (Mott and Jones, 1936). Of course it is assumed that

the impurity scattering is due only to Coulomb interactions.

1.2.4 Detailed Calculation of Current

According to the modern theory of conductivity, the conductivity is given by

$$\sigma = \frac{N_{eff}\, e^2\, \tau}{m} \qquad (3)$$

where N_{eff} is the effective number of conduction electrons, e the electronic charge, m the mass of the electron and τ the relaxation time. In this expression, all the factors are essentially constant except the relaxation time τ which depends on the amplitude of thermal vibrations and the concentration of impurities. The conductivity σ is not explicitly dependent on the temperature. However it depends implicitly on the temperature through the relaxation time τ. Many assumptions were made in order to obtain this result. A study of theory of conductivity will show when we expect equation (3) to be valid.

In the modern theory of conductivity (for instance as outlined by Mott and Jones, 1936) it is possible to calculate the current for an actual metal provided (1) the Fermi distribution is assumed spherical and (2) the transition probability $P(kk')$ for an electron to be scattered from a state k to a state k' is assumed to depend only on

the angle of scattering and not on the initial direction of motion. Here $\vec{k}$ is the wave number of conduction electrons. The electrons are considered as free and assumed to obey Fermi Dirac statistics. Also the scattering is assumed elastic.

The relative filling of available energy states for the electrons is thus given by the Fermi distribution functions

$$f_0 = \frac{1}{\exp (E-F_F)/kT + 1} \qquad (4)$$

where E is the energy of the electrons, E_F the Fermi energy and k the Boltzman constant. In the absence of an external field f_0 is spherically symmetrical and there is no net motion of charge in any direction.

In the presence of an electric field F along the x - direction

$$\left(\frac{df}{dt}\right)_{field} = \frac{df_0}{dE} \frac{dE}{dk} \frac{k_x}{k} \frac{eF}{\hbar} \qquad (5)$$

The effect of the field on the electrons is opposed by the effect of collision between electrons and vibrating atoms or impurities. We therefore have to find the rate of change of f due to collisions. This depends not only on the number of electrons in the initial state k but also on the number of available states around the final state k'.

Similar conditions apply for the reverse process. Therefore

$$\left(\frac{df}{dt}\right)_{coll} = \left[1-f(k)\right] \int f(k') P(k'k)\, dS' - f(k) \int \left[1-f(k')\right] P(kk')\, dS' \quad (6)$$

where dS' is an element of surface in k- space and the integration is over the survace in k-space having the same energy as the initial state k. This expression is obtained when the Pauli exclusion principle is applied rigorously. It is usually assumed that $P(kk') = P(k'k)$ so that equation may be simplified to

$$\left(\frac{df}{dt}\right)_{coll} = \int f(k') P(k'k)\, dS' - \int f(k) P(kk')\, dS' \quad (7)$$

which is the same formula as one obtains without taking into account the exclusion principle. Therefore in this case the Pauli principle has no effect on the conductivity. This may seem surprising but results from our assumptions that the scattering is elastic and $P(kk') = P(k'k)$. There will be a net motion of charge in one direction only if the Fermi distribution is disturbed, i.e. if

$$f = f_0 + g \quad (8)$$

when an external field is applied g increases until the effect of collisions is equal and opposite for the effect of the field. Then g may be defined by

$$g(k) = \frac{df_0}{dk} \frac{k_x}{k} \frac{eF}{h} \tau \quad (9)$$

where the constant τ is the relaxation time. If we substitute for f by $f = f_0 + g$ in equation (7) we obtain,

$$\left(\frac{df}{dt}\right)_{coll} = \left[g(k') - g(k)\right] P(kk') \, dS' \qquad (10)$$

This must be set equal to minus the rate of change due to the field (equation 5). When this is done we finally obtain

$$\frac{1}{\tau} = \int (1-\cos\theta) \quad P(\theta) \quad dS \qquad (11)$$

The reciprocal of the time of relaxation is thus equal to the total probability per unit time that an electron is scattered, with the factor $1 - \cos\theta$ to give extra weight to large angle collisions. Here $P(\theta)$ is the probability of scattering through an angle θ. Hence now we can calculate τ and deduce $g(k)$, the effect of the field and collisions on the distribution function f_0. We can now calculate the current that results from this shifted Fermi function. The contribution to the current per electron is ev_x and the density of electrons in k - space is $\frac{2 f_0(k)}{(2\ )^3}$. The current per unit volume is then

$$j = \iiint ev_x \frac{2f(k)}{(2\pi)^3} \, dk_x \, dk_y \, dk_z \qquad (12)$$

the integration being taken over all k - space. However $v_x = \frac{1}{h} \frac{dE}{dk} \frac{k_x}{k}$ and $f = f_0 - \frac{df_0}{dk} \frac{k_x}{k} \frac{eF}{h} \tau$. The term f_0 gives no contribution to the integral; after changing to

polar coordinates and changing the variable from k to E,

$$j = -\frac{e^2 F}{3 \pi^2 \hbar^2} \int_0^\infty \frac{dE}{dk} \tau k^2 \frac{df_0}{dE} dE \qquad (13)$$

In this equation $df_0/dE = 0$ everywhere except in a narrow band of energies ($\sim kT$) around the Fermi level. So we only have to consider the values of the other variables around the Fermi level. In order to carry out the integration dE/dk and k^2 are usually assumed constant in that region. Also another more important assumption is usually made here. The relaxation time τ is assumed independent of the energy around the Fermi level, i.e. $\tau(E) =$ constant. The integral then reduces to $-\int_0^\infty \frac{df_0}{dE} dE = 1$ and the conductivity is given by

$$\sigma = j/F = \frac{e^2}{3 \pi^2 \hbar^2} \left(\tau k^2 \frac{dE}{dk} \right)_{E=E_F} \qquad (14)$$

$$= \frac{N_{eff} e^2 \tau_F}{m} \qquad (15)$$

where $N_{eff} = \frac{8\pi}{3} \left(\frac{k}{2\pi}\right)^3 \frac{m}{\hbar^2 k} \frac{dE}{dk}$ (16)

Therefore in this approximation the conductivity is not explicitly dependent on the temperature. However it will be seen that if we assume that the relaxation time τ varies

with the energy of the electrons around the Fermi level, i.e. $\tau = \tau(E)$, the conductivity σ will depend explicitly on the temperature.

It is seen from this equation that the conductivity depends on the relaxation time τ_F of the electrons with energies nearly equal to the Fermi energy. If the scattering is isotropic, the relaxation time τ_F equals the mean free time between collisions (see Dekker, Solid State Physics 1958). For this special case we can introduce a mean free path $l_F = v_F \tau_F$ where v_F is the velocity of an electron with the Fermi velocity (which is determined by N_{eff}). For most practical purposes the Fermi energy may be considered constant. Therefore the variation of conductivity with temperature and concentration depends on the mean free path l_F between collisions. This is determined by the various electron-lattice interactions. For example the mean free path decreases as the thermal vibrations increase with temperature. The mean free path is usually long in metals compared to the interatomic distances. This supports the important concept that the resistance is caused only by deviations from periodic potentials in the lattice.

1.3 Resistivity of Dilute Magnetic Alloys

1.3.1 Large Deviations from Mathiessen's Rule

The resistance anomalies of dilute magnetic alloys

will now be described. Much of this information is taken from the recent summary of Gerritsen (1959). The electrical resistivity of these alloys varies with temperature in one of the four ways sketched in Figure 1. Curve A illustrates the normal behavior of dilute alloys. Mathiessen's rule is obeyed. A few dilute magnetic alloys follow this normal behavior. Curves B, C and D illustrate the resistivity anomalies exhibited by many dilute magnetic alloys. Obviously there are large deviations from Mathiessen's rule.

Curve B shows the resistivity minimum exhibited by a few dilute alloys. At very low concentrations ($\approx$0.1 atomic percent) only a minimum of this type is usually seen. Below the temperature of the minimum the resistivity increases down to the lowest temperature observed. e.g. Cu (Co). Usually the temperature of the minimum increases but not linearly with the concentration. In most cases the resistance minimum is below 50° K. However Linde (1958) has observed that the resistance minimum of Au (Va) alloys is above room temperature.

Alloys that have a resistance minimum often have a maximum at lower temperatures. This type of behavior is illustrated by curve C. In the past, this behavior has been observed only in alloys of a monovalent metal containing paramagnetic ions (e.g. Cu (Mn), Au (Fe), Ag (Mn),

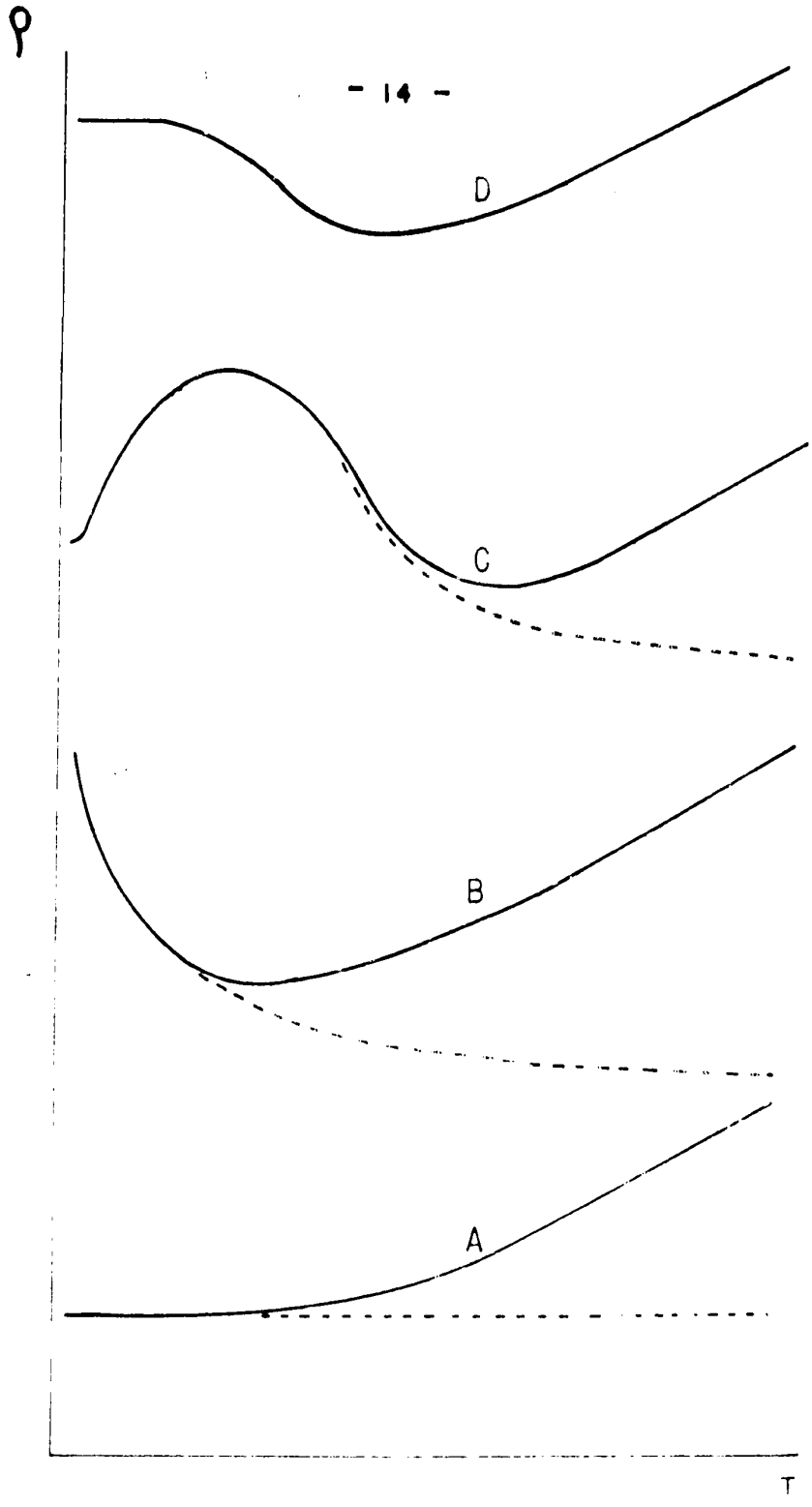

FIGURE 1 - FOUR TYPES OF BEHAVIOR OF THE ELECTRICAL RESISTIVITY OF DILUTE MAGNETIC ALLOYS AT LOW AND VERY LOW TEMPERATURES. THE DOTTED CURVES INDICATE THE FRACTION OF THE RESISTIVITY ATTRIBUTED TO THE IMPURITIES.

Au (Cr), etc.). The resistance maximum of these alloys always has the three following properties; (1) the temperature of the maximum, T_{MAX}, increases rapidly and linearly with concentration, (2) the resistance decreases by a few percent below the maximum and tends to become constant at very low temperatures and (3) the magnetoresistance is negative around the temperature of the resistance maximum. This anomalous magnetoresistance is discussed at the end of this chapter.

Curve D illustrates a resistivity minimum followed by a constant resistivity region at lower temperatures. Such a behavior has been observed in Cu (Fe) and Au (Co) alloys.

At low temperatures the mean free path of conduction electrons is sometimes comparable to the dimensions of the specimen. Without doubt this will have some influence on the resistance measurements (MacDonald, 1956). However these size effects do not seem responsible for the large resistance anomalies just described (MacDonald and Mendelssohn, 1950). These resistance anomalies were observed with specimens of various sizes. Also there is no reason why such effects would occur only in dilute magnetic alloys.

Experiments by Pearson, Rimeck and Templeton (1958) have proven that the resistance minimum is not due to grain boundary effects. A single crystal of Cu (Fe) showed a

resistance minimum just as the polycrystalline specimen did.

It is now nearly certain that the large resistance anomalies just described are genuine properties of dilute magnetic alloys. Therefore these anomalies are properly called deviations from Mathiessen's rule. It is now necessary to establish whether the thermal resistivity or the impurity resistivity is responsible for these anomalies.

1.3.2 Resistivity due to Thermal Vibrations

The resistivity due to thermal vibrations may be different in a pure metal and in its dilute alloys; the impurities may change the characteristic frequency of the lattice. However it does not appear that this effect could account for the large low temperature resistance anomalies of dilute magnetic alloys. According to Mott and Jones (1936), the change in ρ_T due to 1 percent of foreign atoms should be of the order of 1 percent. Also the effect of the impurities on the thermal resistivity should also extend over the whole range of temperatures. Such a small and gradual effect has actually been observed in the resistivity of almost all dilute alloys. (see Mott and Jones, 1936). Moreover if the resistivity due to thermal vibrations was very anomalous in dilute magnetic alloys, there is no evident reason for this discrimination; such an effect should also occur in non-magnetic alloys. However there are no large anomalies

in the resistivity of non-magnetic alloys. Thus we are justified to relate the resistance maxima and minima of dilute magnetic alloys to the impurity resistivity ρ_B.

1.3.3 Anomalous Impurity Resistivity

The large deviations from Mathiessen's rule described in 1.3.1 are attributed to an anomalous impurity resistivity ρ_B. In order to study the impurity resistivity ρ_B it is first necessary to subtract the thermal resistivity ρ_T from the measured resistivity ρ. Let us first consider a resistance minimum of the type described by B, Figure 1. Pearson (1955) has analyzed the resistivity of a Cu (Fe) specimen showing only a minimum. When the subtraction of ρ_T is done, it appears clearly that the very nature of the anomaly is a monotonic increase of the impurity resistivity ρ_B towards lower temperatures. This is indicated by the dotted curve in B, Figure 1. Let us now consider a resistance maximum of the type shown by C, Figure 1. According to recent measurements of Wallingford (unpublished) the impurity resistivity of Mg (Mn) alloys is fairly constant at high temperatures but increases and passes through a maximum at low temperatures. This is shown by the dotted curve of C, Figure 1.

1.3.4 Mechanisms Proposed to Explain the Anomalous Impurity Resistivity of Dilute Magnetic Alloys

There are many ways in which the resistance anomalies may be explained. The impurity resistivity will be anomalous

(a) if the impurities have a particular electronic structure

(b) if magnetic interactions change the scattering cross-section of paramagnetic ions or

(c) if the magnetic ordering of spins increases the periodicity of the lattice (spin-disorder theory).

The mechanisms proposed to explain the anomalous resistivity of dilute magnetic alloys will be reviewed in that order.

(a) Particular Electronic Structure

If the paramagnetic impurities have a particular electronic structure they may produce resonant scattering of conduction electrons with a certain energy (Korringa and Gerritsen, 1953). It may be shown that if the relaxation time $\tau(E)$ depends on the energy of the conduction electrons around the Fermi level, the conductivity will depend explicitly on the temperature (Korringa and Gerritsen, 1953). For example if we take equation (13) and let $\tau = 0$ in two energy bands of width Δ distant by E_1 from the Fermi level, we obtain

$$\frac{\rho}{\rho_0} = 1 + (2\Delta/kT) \exp(E_1/kT) \left\{ 1 + \exp(E_1/kT) \right\}^{-2} \qquad (17)$$

where ρ_0 is the impurity resistivity both at 0^0 K and at high temperatures. By a proper choice of E_1 and Δ, Korringa and Gerritsen could fit this equation moderately well to the resistance maxima of many alloys. However there is no direct evidence for the resonant electronic structure suggested by Korringa and Gerritsen.

Even in very dilute alloys the parameters E_1 and Δ vary with concentration. This is evidently necessary in the curve fitting since the temperature of the maximum increases rapidly with concentration. As the authors point out, this variation of T_{max} with concentration suggests that there is a cooperative phenomenon or interactions between impurities. If the maximum was caused by independent impurities only the magnitude of the effect should increase with the concentration and the temperature of the maximum should remain constant. Korringa and Gerritsen have assumed this to be a cooperative phenomenon between conduction electrons.

In recent years the electronic properties of dilute magnetic alloys have been extensively studied. (Friedel, 1958, and others). It is proposed that there are broadened or "virtual" bound d-states around impurities. This theory is used to explain the deviation from Norbury's Z^2 law. The impurities would be surrounded by concentric shells having alternately an excess or a lack of electrons. This polarisation

could extend to quite a distance from the impurity and align the spins of other impurities. No one has explained how this mechanism could cause the resistance maxima or minima observed in very dilute alloys. Friedel considers these anomalies as still unexplained.

(b) Magnetic Interaction between Impurities

In the absence of fields or other interactions, the impurity resistivity of paramagnetic ions is expected to be constant (Yosida, 1957). However if the paramagnetic ions in solid solution have interactions between themselves, their resistivity will usually vary with temperature. These may be short range or long range interactions but the effect is usually to split the energy levels (e.g. Zeeman levels) of some bound electrons.

Inelastic scattering - Once the energy levels of paramagnetic ions are split, inelastic scattering may occur. By inelastic scattering we refer here to these collisions where the conduction electron excites a bound electron into a slightly different energy level (e.g. Zeeman levels). For the system that causes the scattering this may be an absorption or an emission process. On the other hand the conduction electron loses or gains a small quantity of energy

but more important still, its direction of motion is changed and this increases the resistivity.

The energy states of conduction electrons are all fully occupied except in a range of energies of the order of kT around the Fermi level . Conduction electrons cannot be scattered into fully occupied energy levels. For this reason the resistivity due to inelastic scattering decreases rapidly when kT is approximately equal to the characteristic splitting Δ between energy levels (Schmitt, 1957; Brailsford and Overhauser, 1959). This process is often called the "freezing out" of inelastic scattering and is sometimes used to explain the decrease in resistance below the resistance maximum. (Schmitt, 1956; Dekker, 1959). Also this process is used to explain why the depth of the resistance minimum does not increase as fast as the square of the concentration as required by the pair theory (Brailsford and Overhauser, 1959).

Elastic scattering - The interactions between impurities do not only introduce inelastic scattering but they also make the elastic scattering depend on the temperature.

This is because each energy level of the paramagnetic ion may have a different elastic cross-section and the relative population of the levels changes with the temperature. The relative population of energy levels obeys Boltzmann's statistics and thus the lower energy levels will become more populated at lower temperatures.

In order to account for the increase in impurity resistivity on cooling, it is necessary to assume that the lower energy levels have a larger elastic scattering cross-section. On cooling these energy levels become more populated and the resistance increases (Schmitt, 1956).

Nearest-neighbour pairs of paramagnetic ions may have such a temperature dependent elastic scattering. This has been studied in detail by Dekker (1959) and Brailsford and Overhauser (1959) in their theories on the resistance minimum.

Magnetic susceptibility of dilute magnetic alloys - Some magnetic susceptibility measurements have indicated a gradual transition from a weak ferromagnetism to some type of antiferromagnetism around the temperature of the resistance maximum. J.C. Fisher has suggested that the antiferromagnetism might arise from a weak antiferromagnetic coupling between ferromagnetic domains. Sato, Arrott and Kikuchi (1959) explain the difficulties in interpreting the magnetic

susceptibility measurements on dilute magnetic alloys. They also present objections to the use of the Curie-Weiss molecular field model for dilute alloys and they propose new approaches to the problem. For example there may be important interactions between the nearest-neighbour pairs of paramagnetic ions in the random solid solution.

Later, Dekker (1958) has attempted to explain the magnetic susceptibility of dilute magnetic alloys by postulating antiferromagnetic coupling between the nearest-neighbour pairs and ferromagnetic coupling between the second nearest-neighbour pairs of paramagnetic ions in solid solution. Probably many more measurements will be necessary to obtain a precise knowledge of all the interactions between the paramagnetic ions randomly distributed in the lattice of a parent metal.

Long range interactions between ions - In a paramagnetic substance, each spin finds itself in a fluctuating magnetic field due to neighbouring dipoles. This internal field is of the order μ_B/a^3 where a is a few angstroms, i.e. H_i = 1,000 gausses (cf. Dekker, Solid State Physics, 1958). These dipole-dipole interactions do not seem important in dilute magnetic alloys.

In a random solid solution there may be long-range pseudo-exchange interactions between the paramagnetic ions through the conduction electrons (Pratt, 1957; Yosida, 1957). It is suggested that each conduction electron tends to align the spins of the incomplete d shells in a direction parallel to its own spin (Zener and Heikes, 1953). This will produce a net ferromagnetism if there are more conduction electrons pointing in one direction.

In a dilute alloy, the effect of long-range interactions on one impurity may add up. For example if long-range interactions with other ions split the energy levels of a paramagnetic ion, the magnitude of this splitting may increase with the concentration. In such a case, the inelastic scattering will freeze out at a higher temperature in a more concentrated alloy. This is how Schmitt (1956) explains the increase of T_{max} with the concentration of paramagnetic impurities.

A new mechanism has recently been proposed to explain the antiferromagnetism of dilute magnetic alloys. It involves long-range interactions through spin-density waves (Overhauser, 1960). A theory on the resistance anomalies is soon to follow this one.

Short-range interactions between ions - In a dilute magnetic alloy, the paramagnetic ions are assumed randomly

distributed in the lattice. Therefore a few impurities will be in adjacent lattice sites. In very dilute alloys, the percentage of impurities in pairs is then approximately equal to ve where v is the number of adjacent lattice sites and e is the atomic percent concentration (Dekker, 1959). Therefore in a 0.1% alloy there are approximately 1% of the impurities in pairs if v = 10.

Exchange interactions are often assumed between nearest-neighbour pairs of paramagnetic ions (Dekker, 1959; Brailsford and Overhauser, 1959). These interactions split the energy levels of the d-electrons in the pair and cause temperature dependent elastic and inelastic scattering. In some theories these nearest-neighbour pairs are held mainly responsible for the increase in impurity resistivity below the minimum (Dekker, Brailsford and Overhauser).

Interactions between conduction electrons and ions - The resistivity due to transition element impurities does not obey Norbury's Z^2 law (see section 1.2.3). These deviations may be due to spin dependent interactions between conduction electrons and paramagnetic ions. Norbury's rule is expected to hold only when scattering of conduction electrons is completely due to Coulomb interactions.

In dilute magnetic alloys, we also expect to have exchange interactions between the s-conduction electrons and the unpaired d-electrons of paramagnetic ions (Dekker, 1959; Brailsford and Overhauser, 1959). When the spin of an s-electron points in the same direction as the spin of the d-electron, there is attraction between them (Pratt, 1957). These exchange interactions produce spin-dependent scattering, i.e. the scattering depends on the relative orientation of spins. Both elastic and inelastic scattering may occur.

Besides the above s-d exchange interactions, there may also be important s-s exchange interactions (Brailsford and Overhauser, 1959). These electrostatic exchange interactions are often equated to fictitious magnetic fields (Pratt, 1957).

(c) Spin-Disorder Theory

The spin-disorder theory does not consider the scattering cross-section of one impurity; it only considers the effect of spin orientation on the periodicity of the lattice. This theory is based on the principle that only deviations from a periodic potential produce scattering. According to the spin-disorder theory, any type of magnetic interactions should increase the periodicity of the lattice

and the conductivity.

A naive use of the spin-disorder concept accounts fairly well for the anomalies observed in the resistivity of transition elements (see the review of Coles, 1958). There is a striking resemblance between the resistance anomalies of transition elements and the resistance maximum of dilute magnetic alloys; in each case there is a decrease of the resistance below a certain magnetic-ordering temperature.

1.3.5 Summary of the Theories on the Resistance Anomalies of Dilute Magnetic Alloys

A few of the mechanisms that we have just described are usually included in a theory on the resistance anomalies of dilute magnetic alloys. These theories and some closely related ones are summarized in Table I. Of course this table is too brief to do justice to the theories but it may be useful to compare their basic assumptions, the interactions between ions, the anomalous scattering mechanisms, etc.

As mentioned in Table I, Korringa and Gerritsen, (1953) assume that the impurities have a particular electronic structure producing resonant scattering of conduction electrons. They consider both the resistance maximum, the minimum and the shift in T_{max} with the concentration. However this theory loses much of its appeal since there is

THEORY	Kerringa and Gerritsen (1953)	Schmitt (1956)	Friedel (1958)	Coles' the
MAIN SUBJECT.	The resistance maximum, the minimum and the shift of T_{max} with concentration	The resistance maximum, the minimum and the shift of T_{max} with concentration	Impurity resistivity	Resist
MAIN ASSUMPTIONS	Particular electronic structure of paramagnetic impurities	The scattering cross-section of ions varies due to magnetic interactions between them	Virtual bound d-states	The m order increa perio the l
ION-ION INTERACTIONS		Long-range ferromagnetic interactions possibly via conduction electrons	Long-range ordering via the polarised electron gas	
ANOMALOUS ELECTRON-ION INTERACTIONS	Resonant scattering by impurities	Spin-dependent interactions		Enhan inter
RESISTANCE INCREASE BELOW T_{min}	Resonant scattering	Increase of both the elastic and the inelastic scattering cross-sections of ions		
DECREASE OF RESISTANCE BELOW T_{max}		Freezing out of inelastic scattering		Incre perio the l due t trans
INCREASE OF T_{max} WITH CONCENTRATION	A cooperative electron phenomenon (concentration dependent long-range interactions)	Concentration-dependent long-range interactions between ions		

Table I - Theories closely related to the resistance anom

5)	Friedel (1958)	Coles' sin-disorder theor (1958)	Dekker (1959)	Brailsford and Overhauser (1959)	Overhauser (1960)
axi- and	Impurity resistivity	Resistase maximum	Resistance minimum and maximum	Resistance minimum	Magnetic susceptibility
ress- gne-	Virtual bound d-states	The magnetic ordering of spins increas the periodicity of the latice	Large anoma lous scattering by nearest-neighbour pairs of ions	Large anomalous scattering by nearest-neighbour pairs of ions	Spin-density waves
ma- ons duc-	Long-range ordering via th e polarized electron gas		Exchange interactions between nearest-neighbour ions	Exchange interactions between nearest-neighbour ions and long-range pseudo-exchange interactions	Long-range antiferromagnetic order ing through spin-density waves
t s		Exchang interactions	Exchange interactions between s-electrons and pairs	Exchange interactions between s-electrons and pairs	
the ring			An increase of the elastic scatter ing cross-section of pairs	Increase of the elastic scattering cross-sect'n of pairs opposed by a freezing out of the inelastic scattering due to "isolated" ions	A theory on the anomalous resis tance is to appear soon
		Increas in the periodicity of the latice due to a magnetic transition	Freezing out of inelas t ic scattering and possibly a decrease of the elastic scattering due to pairs		

ns

ated to the resistance anomalies of dilute magnetic alloys.

no direct evidence for the particular electronic structure postulated. The theory of Friedel (1958) continues along similar lines but only succeeds in explaining the deviations from Norbury's Z^2 law; to date the low temperature anomalies remain unexplained.

The theory of Schmitt (1956) is on the resistance maximum, the minimum and the shift of T_{max} with concentration. He relates the anomalous resistance to the magnetic interactions in the alloy. However, due to a lack of detailed information, his theory is based on a very simple magnetic model. Also the calculations of scattering involve many assumptions. According to this theory the decrease in resistance below T_{max} is due to the freezing out of inelastic scattering.

Dekker (1959) and Brailsford and Overhauser (1959) use a similar approach as Schmitt but they study mainly the scattering of nearest-neighbour pairs in relation to the resistance minimum; the resistance maximum is briefly mentioned by Dekker. In these two theories, there is no reference to the shift of T_{max} with concentration. The interactions between nearest-neighbour ions are independent of the concentration. Therefore the nearest-neighbour pairs could not easily account for the increase of T_{max} with increasing concentration.

Coles proposes an interesting explanation of the resistance maximum: the spin-disorder theory. However in dilute magnetic alloys there is not only "spin-disorder"

due to the random orientation of spins but there is also an intrinsic "spatial disorder" due to the random distribution of ions in the lattice. Because of this spatial disorder it is less probable that the spin-disorder theory is adequate for dilute magnetic alloys.

Theoretical physicists apparently agree that the scattering of conduction electrons is spin dependent. However there is no agreement

(1) on the detailed mechanisms of magnetic interactions between ions in dilute magnetic alloys

(2) on the importance of nearest-neighbour pairs in these anomalies

(3) on the cause of the resistance decrease below T_{max}; is it the freezing out of inelastic scattering, a decrease of the elastic scattering cross-section due to magnetic interactions or an increase in the periodicity of the lattice with the spin-ordering?

1.4 Magnetoresistance of Normal Dilute Alloys

Normally the electrical resistance of a metal or an alloy increases in a magnetic field. This increase is believed to depend primarily on the ratio l/r where l is the mean free path of conduction electrons and r is the radius of their circular motion in a magnetic field (for

instance see the review of MacDonald and Sarginson, 1952).

1.4.1 Kohler's Rule

It was shown by Kohler that the dependence of magnetoresistance on temperature, magnetic field and purity of the sample should be a function of $H\tau$ alone. Kohler's rule has a fairly simple theoretical basis (for example see Ziman, 1960). Since the relaxation time τ is inversely proportional to the electrical resistivity ρ, Kohler's rule is commonly written

$$\frac{\Delta\rho}{\rho} = F\left(\frac{H}{\rho}\right) \qquad (18)$$

where F is a single function valid for all dilute alloys of one metal, all temperatures and magnetic fields intensities. As far as Kohler's rule is concerned F may be any function of H/ρ. However for one alloy system it should be the same function F for all temperatures and dilute concentrations. By plotting $\Delta\rho/\rho$ as a function of H/ρ for various temperatures and purities, all points should fall on the same curve.

If an alloy system obeys Mathiessen's rule and we can neglect thermal expansion, the Kohler rule may be written

$$\frac{\Delta\rho}{\rho} = F\left(H \times \frac{R_{273} - R_{4.2}}{R_T}\right) \qquad (19)$$

where R_T is the resistance at temperatures T, R_{273} is the resistance at 273° K and $R_{4.2}$ is the residual resistance at 4.2° K.

When the magnetoresistance of only one specimen is studied at different temperatures, it is sufficient to use the relation

$$\frac{\Delta\rho}{\rho} = F\left(H \times \frac{R_{273}}{R_T}\right)$$

Usually the magnetoresistance of non-magnetic dilute alloys is fairly well described by Kohler's rule even at low temperatures (Gerritsen, 1953; Yntema, 1953).

1.4.2 Further Remarks on Magnetoresistance

According to Justi metals can be divided into two groups as far as the magnetoresistance is concerned. Metals with an odd valency (e.g. Na, Cu, Au, Al, In) have a magnetoresistance that increases more slowly than H^2/R^2 for moderate values of H and as found by Kapitza, shows signs of saturating in high magnetic fields. On the other hand metals with an even valency (e.g. Mg, Zn, Be, Pb) have a magnetoresistance $\Delta R/R$ that increases nearly as H^2/R^2. According to Wilson this behavior is in good agreement with the calculation of magnetoresistance based on the two-band model.

For purposes of measurement, it is the ratio $\Delta R/R$ that is important. However considering only ΔR gives a

better idea of the effect due to a magnetic field. For example for Mg, ΔR is approximately proportional to H^2/R. Therefore for a constant magnetic field, ΔR increases as R decreases towards low temperatures. Also it is evident that the addition of impurities increases R and decreases ΔR. This effect of impurities is particularly important at low temperatures where the resistivity due to thermal vibrations is negligible.

1.5 Magnetoresistance of Dilute Magnetic Alloys

1.5.1 Deviation from Kohler's Rule

Often, the magnetoresistance of dilute magnetic alloys does not obey Kohler's rule. (Gerritsen 1953; Webber, 1956). At temperatures below the resistance minimum the magnetoresistance does not increase as rapidly as predicted by Kohler's rule. Also the magnetoresistance even becomes negative around the temperature of the resistance maximum. Gerritsen (1953) has suggested the following classification:

(1) metals having a normal resistance and obeying Kohler's rule,

(2) metals with a resistance minimum and obeying Kohler's rule,

(3) metals with a resistance minimum and maximum and not obeying Kohler's rule.

However according to recent measurements, this classification does not hold (Gerritsen, 1959). Some alloys that show only a resistance minimum have a negative magnetoresistance e.g. Cu (Co), Cu (Ni). It seems that when sufficient paramagnetic impurities are present, Kohler's rule always breaks down.

The measurements of Korringa and Gerritsen show (1) that the negative magnetoresistance may be a relatively large effect. A decrease of 25% in a field of 20 kOe was observed in the resistance of Ag containing 0.1 atomic percent Mn. (2) The negative magnetoresistance saturates in high magnetic fields and (3) the negative magnetoresistance does not increase indefinitely with the increase of concentration. The highest percentage decrease is found with moderately dilute alloys.

1.5.2 Polarisation of Spins by an External Magnetic Field

An external magnetic field has nearly no polarisation effect on the spins of conduction electrons. They behave as a classical gas with a characteristic temperature of the order of 10,000° K and their paramagnetism is of the order of 100 times smaller than for free ion spins.

However an external magnetic often has an appreciable effect on the spins of paramagnetic ions. The transition

element impurities usually become paramagnetic ions when they are dissolved in a metal. Quite often the orbital magnetic moment of the ion is quenched by the electrical fields of the lattice. In such cases only the unpaired d-electron[5] contribute to the paramagnetism. When the spin-orbit coupling is negligible, Curie's law describes the paramagnetism of ion spins at high temperatures and in weak fields. However, ordinary magnetic fields are often sufficient to approach saturation conditions at liquid helium temperatures; the quantity $\mu H/k \approx 1^{\circ}$ K when H equals 10 kOe. Under these conditions Curie's law is no longer valid and the magnetization may be described by the Brillouin function (Korringa and Gerritsen, 1953).

1.5.3 Theories on the Negative Magnetoresistance

The anomalous magnetoresistance of dilute magnetic alloys may be regarded as the sum of two effects; (1) a normal resistance increase due to the effect of the magnetic field on the conduction electrons (2) a decrease of the resistance due to the effect of the magnetic field on the impurities (Korringa and Gerritsen, 1953). The observed magnetoresistance will be positive or negative, depending on which effect predominates.

Just as for the anomalous zero field resistance, negative magnetoresistance has received various explanations. The external magnetic field may change the elastic and inelastic scattering cross-sections of the paramagnetic ions (Schmitt, 1956; Dekker, 1959). Also the external magnetic field may increase appreciably the periodicity of the lattice by aligning the spins of paramagnetic ions (Coles, 1957). By using the first approach Ziman (1960) proves that the negative magnetoresistance should vary as the square of the magnetisation; such a behavior has actually been observed for Cu (Co) alloys (Jacobs and Schmitt, 1953).

There are various explanations of the negative magnetoresistance but in each theory it is assumed that all the paramagnetic ions take part in this phenomenon and not only a small fraction of the impurities like the nearest-neighbour pairs.

CHAPTER 2

2.1 Introduction

In this chapter we describe the apparatus and methods for the measurement of electrical resistance down to very low temperatures and of the magnetoresistance at liquid helium temperatures. First the cryostat is described and then details are given on the mounting of the resistance specimen and paramagnetic salt for cooling by adiabatic demagnetization (sections 2.2 and 2.3). Sections 2.4 and 2.5 are on the paramagnetic salts and the measurement of temperature below 1°K.

The measurement of electrical resistance is described in section 2.6 which includes a description of the galvanometer amplifier used to measure small voltages. The next section is on the measurement of magnetoresistance.

The precision of measurements is discussed throughout the chapter and these discussions are summed up in section 2.8. The chapter closes with section 2.9 on the preparation of Mg (Mn) specimens.

2.2 Cryostat

The photograph of the cryostat (figure 2(a)) shows part of the high vacuum system, the liquid air and liquid

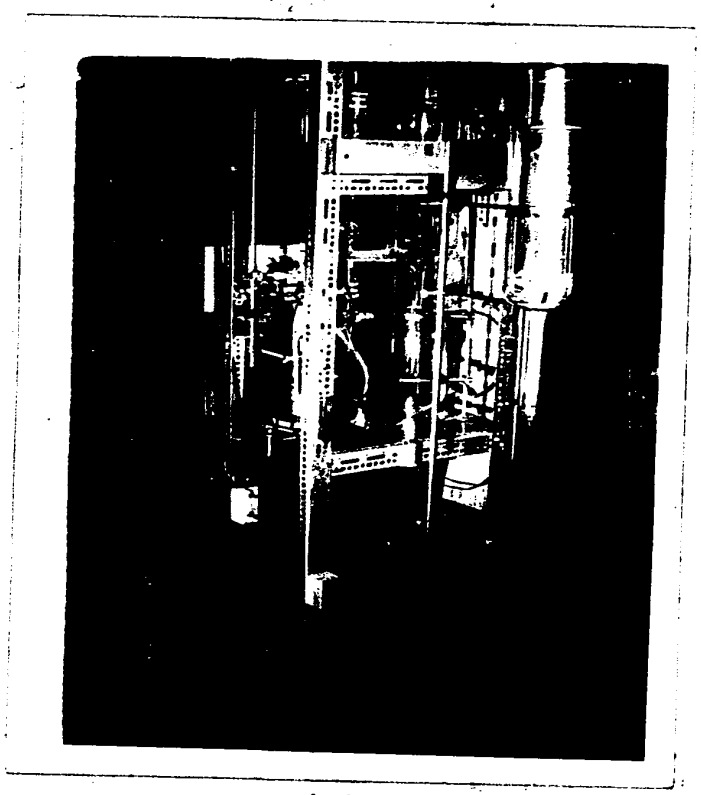

(A)

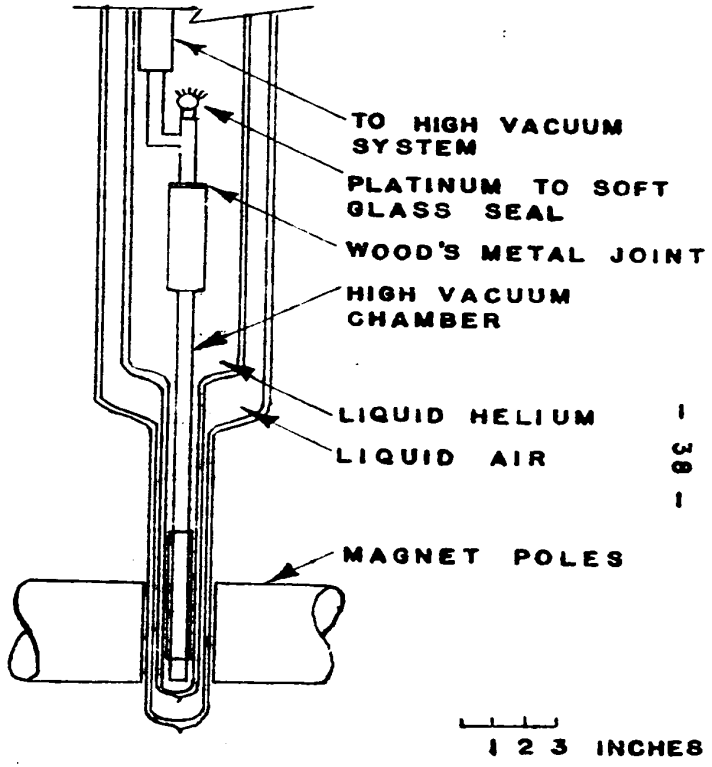

(B)

FIG. 2 — (A) PHOTOGRAPH OF CRYOSTAT AND (B) DETAILS OF MAGNET, DEWARS AND HIGH VACUUM CHAMBER.

helium dewars in which the investigations are done. The vacuum system in which the resistance specimen and the paramagnetic salt are suspended is sketched in figure 2 (B). A cross-section of the two dewars is also seen in this sketch. Above the vacuum chamber there is a platinum to soft-glass seal with platinum wires to bring out the electrical signals and a radiation trap to reduce the heat leaks to the specimen.

2.2.1 Liquid Helium Temperatures

The resistance measurements discussed in this thesis were taken at liquid helium temperatures from 4.2°K to about 1.3°K and below liquid helium temperatures down to about 0.2°K by adiabatic demagnetization of a paramagnetic salt. These two ranges of temperature will be discussed separately.

The temperatures from 4.2°K to about 1.3°K are obtained by lowering the vapour pressure of liquid helium with a large mechanical pump that has a speed of 60 litres per second. The pumping line to the cryostat is 3-1/2 inches in diameter except near the cryostat where this diameter is reduced to 2 inches and finally to 1 inch at the dewar cap. At temperatures above the lambda point of helium the vapour pressure is measured directly by a mercury manometer. Below the lambda point, a more sensitive n-dibutyl phtalate manometer is used. The absolute temperature is then obtained

from the vapour pressure by means of the 1958 scale (Brickwedde, 1958).

We estimate that by the visual reading of the manometer, the liquid helium temperatures are measured with an accuracy of $\pm$ 0.01°K. During an experiment, about four resistance and four temperature readings are alternately taken around one temperature. It takes about 3 to 4 minutes to take these readings and during that time the temperature of the helium bath is allowed to decrease by about 0.1°K. These groups of four readings are then averaged. The accuracy of the average temperature is comparable to the accuracy of a single temperature reading provided the rate of decrease of the temperature and the time between readings are constant. With a little practice these conditions are fairly well achieved.

We would like to give a word of caution to the reader. Above the lambda point, liquid helium has a small thermal conductivity and some other mechanism must help to keep temperature homogeneity in the helium bath. During the pumping, fast moving bubbles help to keep the temperature constant throughout the bath. However, we have observed on many occasions that if the helium bath is left to warm up slowly by itself, the bottom of the bath may still be around 2.5°K when the top reaches 4.2°K and it may take hours before this temperature gradient is destroyed. This effect is

sometimes mentioned in the literature but we were surprised by its large magnitude.

2.2.2 Cooling below 1°K

In order to take resistance measurements below the temperature of the helium bath, the metallic specimen is placed in contact with a paramagnetic salt which is magnetized isothermally and demagnetized adiabatically with the resulting cooling. Helium exchange gas is used for the isothermal process. Adiabatic conditions are obtained by evacuating the exchange gas from the vacuum chamber, down to a pressure of the order of 10^{-6} mm of mercury as indicated by a commercial Philips gauge. To achieve such pressures, we use a single stage mercury diffusion pump backed by a Duo Seal mechanical pump. This high vacuum system also includes facilities to let the helium exchange gas into the vacuum chamber.

The vacuum chamber in the helium bath is made from a thin brass tube permanently sealed at one end. The top of this tube joins to the vacuum system by means of a Wood's metal seal. This seal is easily undone to remove the sample chamber and change the specimen.

The adiabatic demagnetizations were done around 1.3°K from fields of about 5 kOe. With the salts used, the temperature dropped to about 0.2°K when this field was

removed. The salt and the metallic specimen then warmed up to the bath temperature in a period which was found to vary from 20 minutes to two hours in different runs. The heat leak to the salt depends on the amount of exchange gas present, on the vibrations transmitted to the salt, on the radiation and on the threads used in the suspension, all factors which cannot be accurately controlled. During the warm up time the temperature of the salt and the resistance of the metallic specimen are measured alternately about every half minute.

2.3 Mounting of the Resistance Specimen and Paramagnetic Salt

A diagram to illustrate the mounting of the resistance specimen and of the paramagnetic salt is shown in figure 3. The specimen and the salt are held rigidly by a single nylon thread from above and one from below. These two lengths of thread are attached to a cage or support over which the vacuum chamber slips into place. The cage is made from a thin brass tube cut in half along its axis.

The resistance specimen must be wound around a support that is rigid, electrically insulated and which also provided a good thermal contact with the refrigerant. Also the specimen support must have about the same thermal expansion as the specimen itself if mechanical strains are to be avoided

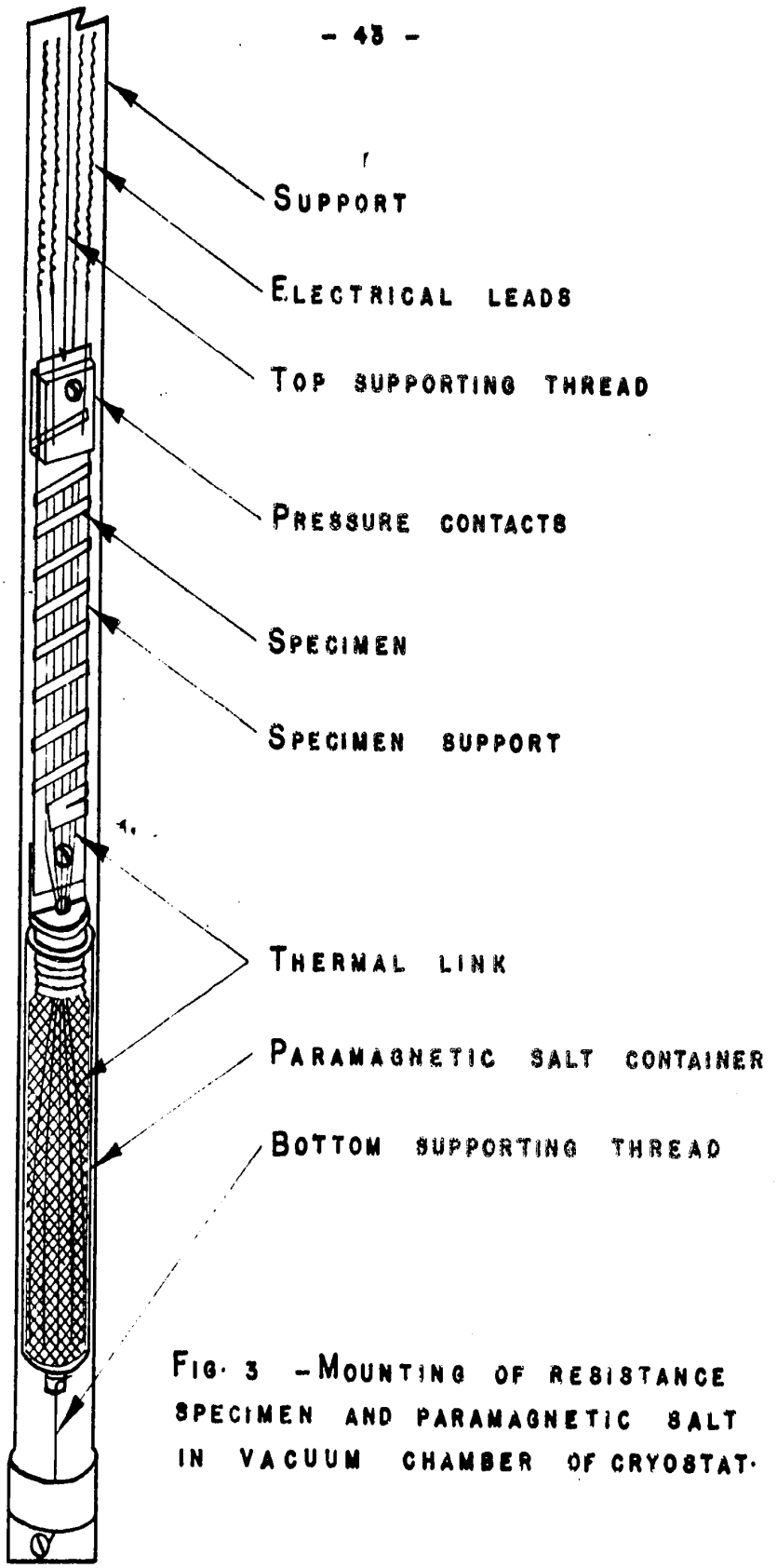

FIG. 3 - MOUNTING OF RESISTANCE SPECIMEN AND PARAMAGNETIC SALT IN VACUUM CHAMBER OF CRYOSTAT.

on cooling. After investigating various types of support, the following one was adopted. A magnesium plate 1 cm wide, 1.5 mm thick and 8 cms long is screwed against the copper cap of the paramagnetic salt container. This plate is electrically insulated with varnish and cigarette paper. Some 400, No. 40 (B and S) enamelled copper wires imbedded in the paramagnetic salt come out of the copper cap. These wires are separated into two bundles about 5 cm long that are pressed and glued on each side of the magnesium plate by means of insulating varnish.

The resistance specimen in the form of a long thin and narrow strip or ribbon, is wound non-inductively around the specimen support just described. Then it is covered with glyptal varnish to insure thermal equilibrium and mechanical rigidity.

The resistance measurements involve the determination of the voltage drop across the specimen when a known current is flowing through it. It is quite essential to have separate current and voltage contacts on the specimen. Pressure contacts are very satisfactory for Mg specimens. Our pressure contacts consist of 2 short lengths of No. 24 (B and S) copper wires pressed against each end of the specimen. Two 1/16 inch thick lucite plates and a screw form a miniature vice that presses the copper wires against the specimen.

Long super conducting leads are soldered to the base copper wires pressed on the specimen. The other end of these super conducting wires are soldered to platinum wires that bring the electrical signals in and out of the high vacuum chamber through a platinum to soft-glass seal. When the specimen is cooled below 1.3°K, these super conducting leads have a small thermal conductivity and hence do not conduct much heat from the liquid helium bath to the specimen and salt.

2.4 Paramagnetic Salts and the Salt Container

We have used both chrome alum and iron ammonium alum for cooling below 1°K by adiabatic demagnetization. Temperatures near 0.2°K were attained. The iron ammonium alum gave slightly lower temperatures.

The chrome alum usually loses some water of hydration during storage and is therefore recrystallized before an experiment.

In order to improve the thermal contact between the salt and the copper wires (thermal link), a few drops of an eutectic mixture of glycerol and water are mixed with the salt. This eutectic mixture consists approximately of 16 cc of glycerol with 4 cc of water.

The salt container is a thin-wall lucite cylinder with a copper cap screwed at one end. Besides the copper

wires acting as thermal link, this lucite cylinder contains about 6 grams of salt. The copper wires are distributed through the salt and come out of the container through a hole in the copper cap.

A metal container for the salt has previously been tried but without success. It was sealed with super conducting solder that disrupted the measurements of the magnetic susceptibility of the salt.

It will be explained (see section 2.5.3) that in these indirect cooling experiments, there is no advantage in using an ellipsoidal salt container instead of a cylindrical container. In some other types of experiments, an ellipsoidal salt sample increases the accuracy of temperature measurements below $1^{\circ}K$.

2.5 Measurement of Temperature Below $1^{\circ}K$

Below $1^{\circ}K$, the magnetic susceptibility of the paramagnetic salt is used as a thermometric parameter. This susceptibility is measured by means of a Hartshorn bridge. We assume that the specimen is in thermal equilibrium with the salt and this has been verified qualitatively by means of a carbon resistor.

2.5.1 Thermal Equilibrium

We have taken great care to provide a good thermal

link between the resistance specimen and the cooling salt (see sections 2.3 and 2.4). Moreover the current through the specimen was kept small so that the Joule heating did not exceed 1 erg/minute. The behaviour of the specimen resistance and of a carbon thermometer indicated qualitatively that the specimen cooled to the temperature of the salt in less than a minute after the adiabatic demagnetization.

2.5.2 Susceptibility Bridge

We measure the magnetic susceptibility of the paramagnetic salt by means of an unbalanced Hartshorn bridge. A primary and a secondary coil are wound outside the vacuum chamber in which the paramagnetic salt is suspended. A large direct current is reversed in the primary coil and it induces in the secondary coil a current proportional to the susceptibility of the salt. This induced current is measured by a ballistic galvanometer. The circuit of the bridge is shown in figure 4. This direct current bridge is preferred to a-c bridges because it produces less eddy current heating. Eddy currents may be quite large in metallic conductors at low temperatures.

The current in the primary coil is measured by means of a precision ammeter (E. Turner Co.) that may be read to $\pm$ 0.2%. The bridge is balanced by means of a

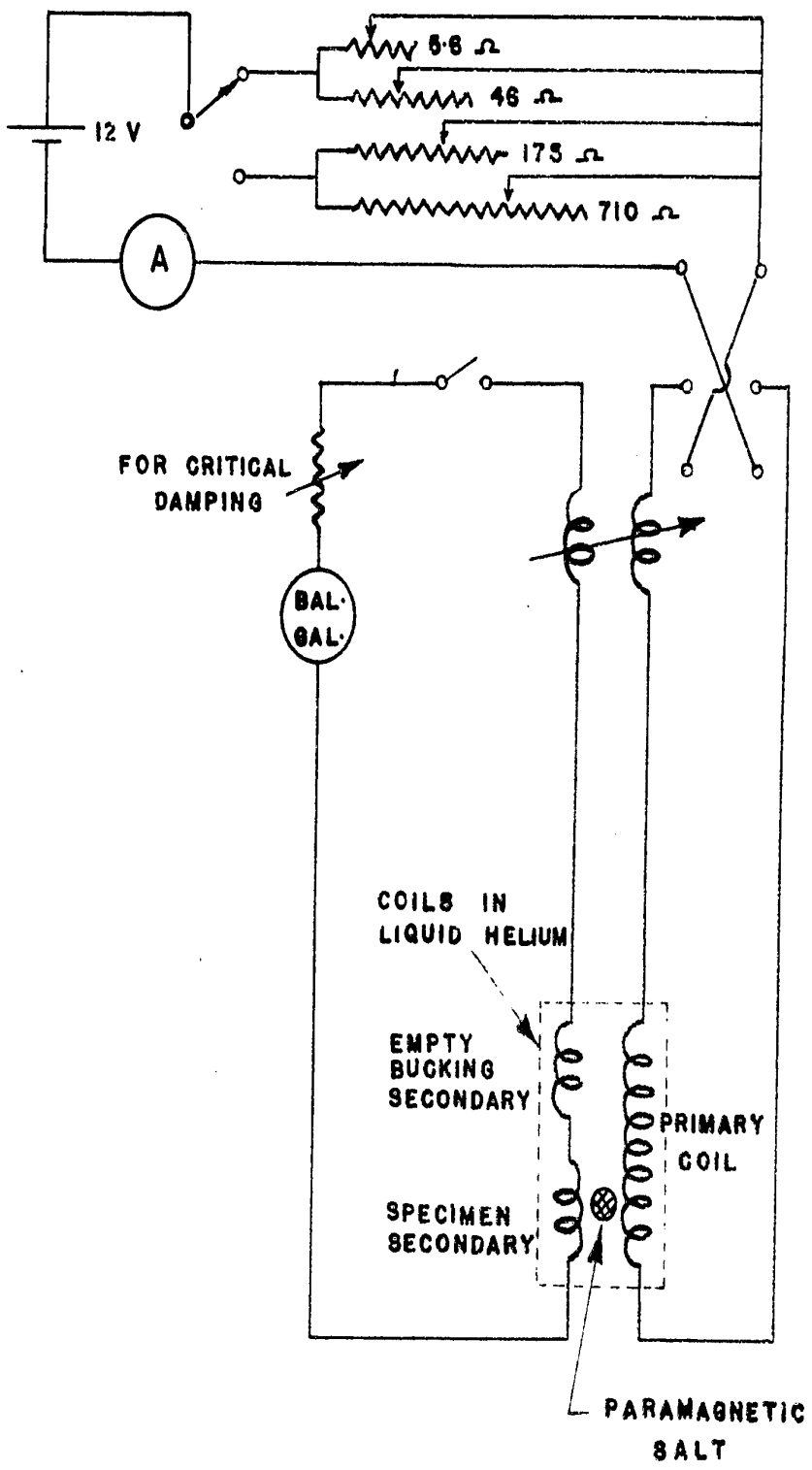

FIG·4 – DC CIRCUIT AND INDUCTION COILS TO MEASURE THE MAGNETIC SUSCEPTIBILITY AT LOW AND VERY LOW TEMPERATURES.

variable mutual inductance (1 mh General Radio).

The ballistic galvanometer has a sensitivity of 1,500 mm/ μA at 2 metres, a resistance of 15 ohms and a period of 22 seconds. A decade resistance box in series with the galvanometer provides critical damping. It is possible to take susceptibility readings about every half minute.

Because of floor vibrations it is necessary to place the ballistic galvanometer on a special support. A modified Julius suspension (cf. Strong, 1950) is used with success. This suspension does not transmit to the galvanometer the damaging horizontal, high frequency vibrations from the floor. The Julius suspension has a low natural frequency (about 0.5 cycles/second) and is loosely coupled to the floor. A photograph of the galvanometer and Julius suspension is shown in figure 5.

Details of the susceptibility coils are seen in figure 6. It will be noticed that the secondary winding is in two parts that are wound in opposite directions. One part of the secondary is placed around the salt. The other part is placed higher than the salt and cancels most of the temperature independent signal of the first part. This bucking increases greatly the sensitivity of the bridge. Otherwise a very large current would pass through the

Figure 5 - Modified Julius suspension for the ballistic galvanometer.

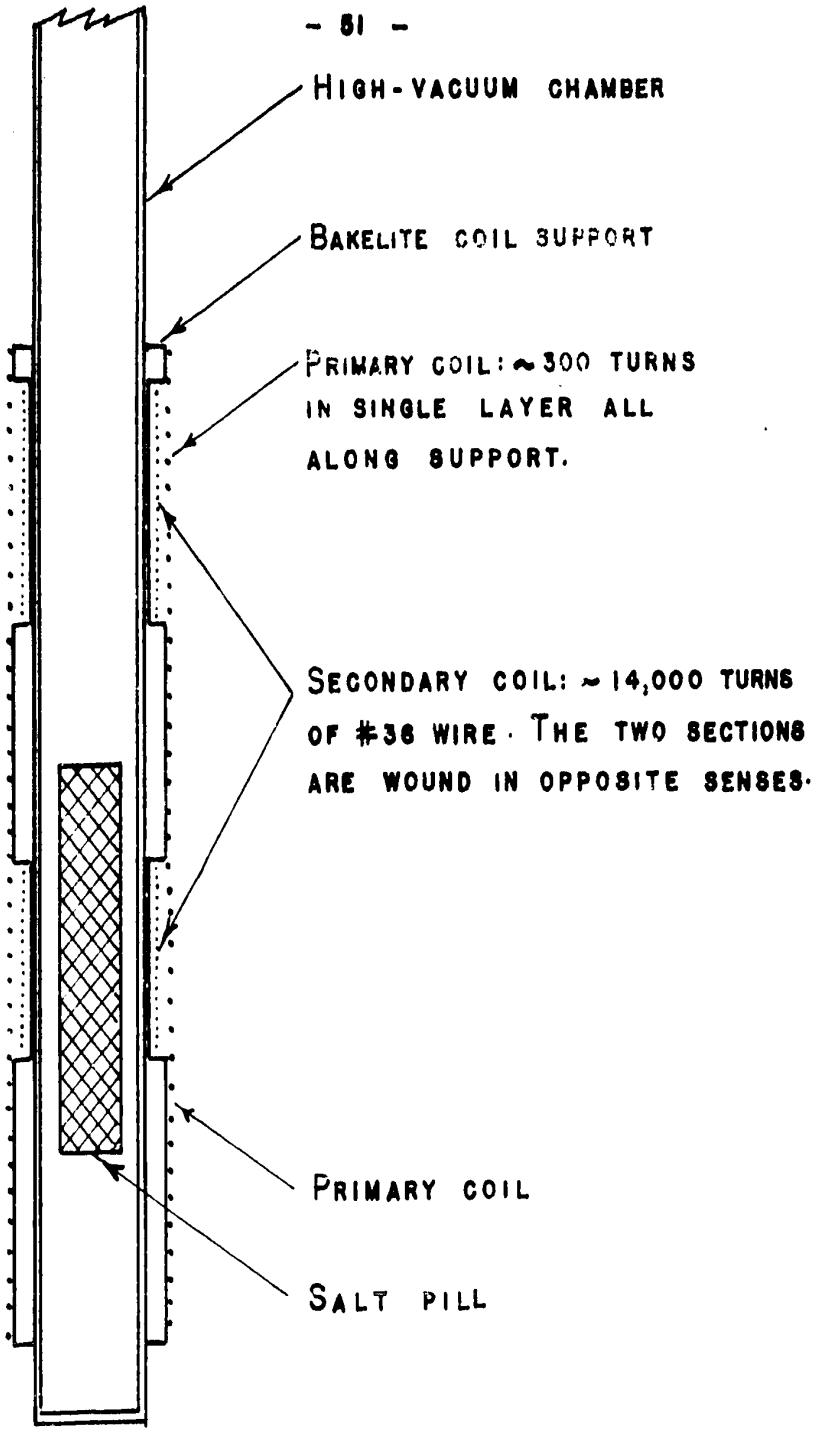

FIG. 6 - SCALE DRAWING OF SUSCEPTIBILITY COILS AND THEIR POSITION AROUND THE VACUUM CHAMBER.

ballistic galvanometer and the relative change would be small on cooling the salt. It is better to do most of this bucking in the helium bath because then, the resistance of the secondary circuit can remain relatively low in spite of its large inductances.

The primary current of the susceptibility bridge is easily kept constant to about ± 1%. Also the diflections of the ballistic galvanometer may be read to about ± 1%. So the susceptibility bridge has a precision of about ± 2%.

2.5.3 Magnetic Susceptibility of the Salt Sample

Below 1°K the magnetic susceptibility of the paramagnetic salt is used as a thermometric parameter. The susceptibility bridge is calibrated at liquid helium temperatures where Curie's law is usually valid and may be written as

$$\chi_{ext} = \frac{C}{T}$$

where χ_{ext} is the susceptibility defined by M/H_{ext}. M is the magnetic moment and H_{ext} the field in the solenoid. C is the Curie constant and T the absolute temperature of the helium bath and salt. When extrapolated below 1°K this equation gives the magnetic temperature T^*, i.e.

$$\chi_{ext} = \frac{C}{T^*}$$

However if the magnetic temperature is measured very precisely, the results will depend on the shape of the salt sample used. Instead of the above equation it is necessary to use

$$\chi_{ext} = \frac{C}{T^{\Theta} - \Delta}$$

where Δ is a correction that depends on the shape of the sample and the interaction[5] between the paramagnetic ions. In the Lorentz approximation,

$$\Delta = \left(\frac{4\pi}{3} - \varepsilon\right) f \frac{C}{V}$$

where $4\pi/3$ is related to the Lorents internal field, ε is the demagnetizating factor dependent on the shape of the salt sample, f is the filling factor and C/V is the Curie constant of the salt per unit volume. When it is possible Δ is calculated and the corrected magnetic temperatures T^{Θ} below $1^{\circ}K$ are given by the extrapolation

$$\chi_{ext} = \frac{C}{T^{\Theta} - \Delta}$$

The Δ correction is such that for a sphere $\Delta = 0$. For this reason T^{Θ} is called the magnetic temperature of a spherical salt sample. It is possible to calculate precisely the demagnetization factor ε and hence Δ for an ellipsoid or a sphere. In some experiments with a salt only, we have used an ellipsoidal plastic container with a 4/1 axis ratio.

The Δ correction was about $0.02^{\circ}K$ for chrome alum and $0.05^{\circ}K$ for iron ammonium alum. The lowest temperatures attained on demagnetizing agree with the initial conditions and the data in the literature.

However when the salt is used for cooling a resistance specimen, the copper wires used as a thermal link effect the distribution of salt in an unpredictable manner. Also the filling factor f is not known exactly. Therefore, when taking resistance measurements, it does not seem useful to use an ellipsoidal salt sample and to estimate the Δ -correction for the magnetic temperature below $1^{\circ}K$. Therefore a simple cylindrical plastic container is used and the Δ -correction is completely neglected. All the data in the literature is given in terms of the corrected magnetic temperature $T^{\circledast}$. Therefore in this case it is not possible for us to make the conversion from the uncorrected temperature $T^{\#}$ to the absolute temperature T ($^{\circ}K$). However it may be shown that the Δ -correction and the conversion to absolute temperatures are two corrections of about the same magnitude (0.05° for iron ammonium alum) and sometimes opposed to each other. Therefore the error in neglecting both of them remains quite small. The error is of the order of $\pm\ 0.05^{\circ}K$ at the lowest temperatures for the salt samples we have used.

2.5.4 Calibration of Susceptibility Bridge

The susceptibility bridge is calibrated at liquid helium temperatures. A primary current of about 500 mA is used. This produces a field of about 10 gausses inside the primary coil. This field is not large enough to produce saturation effects so that Curie's law is valid.

The bridge is balanced at $4.2^{\circ}K$ by means of the variable inductance. A few deflections of the ballistic galvanometer are taken at five or six temperatures from $4.2^{\circ}K$ to $1.3^{\circ}K$. These readings are averaged for each temperature and δ is plotted versus $1/T$. As it was explained in section 2.5.3, the Δ correction is completely neglected for resistance measurements. This graph gives a straight line defined by

$$\delta = \frac{A}{T} + B$$

where A is the slope of the line and B the intercept along the δ-axis. These constants are determined from the graph.

Before adiabatic demagnetizations, the primary current is reduced to 100 mA to avoid excessively large deflections. By extrapolating the above calibration for the reduced current, the uncorrected magnetic temperatures below $1^{\circ}K$ are given by

$$T^{*} = \frac{A}{5\delta' - B}$$

where the factor 5 accounts for the decrease in the primary current and δ' is the deflection of the ballistic galvanometer with the reduced primary coil current. From this equation, T^{*} is calculated for a few values of δ' and plotted on a graph. A continuous parabolic curve is drawn through these points and the temperatures below $1^{\circ}K$ are conveniently read from this graph for the ballistic galvanometer deflections observed.

A calibration done in the above manner is fairly accurate. The temperature of the helium bath is measured to $\pm 0.01^{\circ}K$ and, the susceptibility bridge has a precision of about $\pm$ 2%. However this introduces only a small error in the calibration since a straight line is passed through five or six calibration points and each point is an average of four sets of readings.

The errors in bridge measurements taken below $1^{\circ}K$ introduce negligible errors in the temperature measurement. This may be seen by differentiating the extrapolation equation with respect to δ'. We then find that

$$\frac{dT^{*}}{T^{*}} = \frac{d\delta'}{\delta' - B/5}$$

If B = 0, the percentage error in the magnetic temperature below 1°K equals the percentage error of the ballistic bridge. Thus an error of about 2% of the ballistic bridge causes an error of only 0.01°K at 0.5°K. This is negligible compared to the error of about ± 0.05°K caused by neglecting the Δ-correction and the conversion from magnetic to absolute temperatures.

2.5.5 Carbon Resistors as Thermometers Below 1°K

As previously mentioned, secondary thermometers may be very useful below 1°K to verify thermal equilibrium, etc.. Dilute alloys with a resistance minimum maybe used but their resistance is small and also their sensitivity is quite low. Croft and his co-workers (1953) have measured only a 3% increase in the resistance of a long gold wire from 1°K to 0.1°K. Up to now mainly Allen-Bradley carbon resistors have been used below 1°K. Their resistance may increase from 1000 ohms at 1.3°K to 1 megohm at 0.3°K. In fact this resistance increase is nearly too large for convenient measurements.

We have tried to calibrate carbon resistors at liquid helium temperature and extrapolate these results for the measurement of temperature below 1°K. Clement et al (1953) suggest the extrapolation equation

$$\log R + K/\log R = A + B/T$$

A plot of log R + K/log R vs 1/T gives the constants A and B. This extrapolation equation did not give us satisfactory results. It just indicated qualitatively that cooling occurred. It seems that such an extrapolation is just an informed guess. The manner in which the resistance is measured may be very important. For these reasons it seems that carbon resistors are reliable below $1^{\circ}K$ only if they are calibrated at those temperatures against magnetic temperatures. Also their resistance must be measured in the same manner as during their calibration. Even then, the results might not be exactly reproducible.

The resistance of carbon thermometers increases so much below $1^{\circ}K$ that most resistance bridges are not practical. We have used a simple method of measurement. A small current is passed through the resistor and the voltage drop across the resistor is measured directly by a student potentiometer. At $1.3^{\circ}K$ the thermometer current is reduced from 50 to 1 μA to avoid heating. Below $1^{\circ}K$ the resistance of the carbon thermometer increases so much that the current in the circuit decreases appreciably and a correction must be made.

2.6 Measurement of Electrical Resistance

2.6.1 Method

The electrical resistance is measured by passing a direct current through the specimen and measuring the voltage drop across it. Long specimens are used to increase the voltage drop IR without increasing too much the Joule heating equal to I^2R. This is important below $1^\circ K$ to avoid warming the specimen above the temperature of the salt. A typical specimen may have a resistance of 0.05 ohms at $4.2^\circ K$ and with a current of 200 microamperes the Joule heating is then 1.2 ergs/minute. In one particularly good experiment with only a paramagnetic salt, the total heat leak was calculated to be approximately 60 ergs/minute around $0.2^\circ K$. So in such a case 1 erg/minute of Joule heating would have a negligible effect on the warm up time. However it is a safe value to be more certain of thermal equilibrium.

The source of current is shown in figure 7. The current is verified by means of a standard resistor and a potentiometer. During an experiment the current is frequently verified and is usually found to vary by less than 0.1%.

In the example given above the voltage drop across the specimen is of 10 microvolts. This voltage

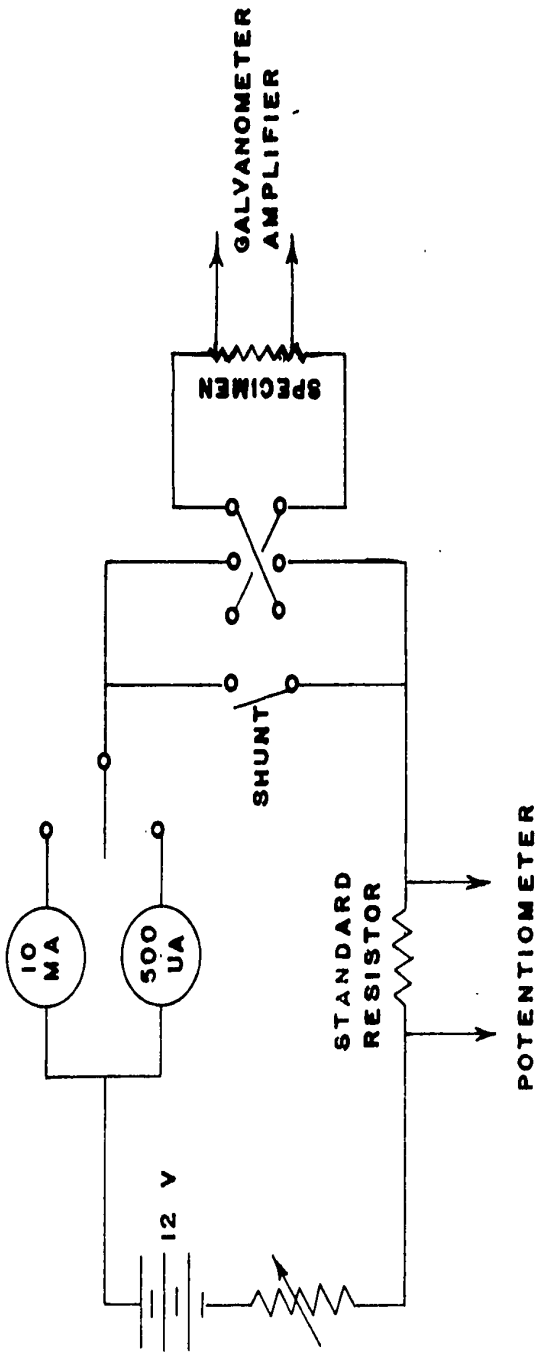

FIG. 7 - CURRENT SOURCE OF SPECIMEN.

may be measured precisely by means of the galvanometer amplifier described by MacDonald (1956).

2.6.2 Galvanometer Amplifier

The circuit of the galvanometer amplifier is shown in figure 8. A beam of light reflected from the mirror of the primary galvanometer G_1 falls equally on two photovoltaic cells. The application of an input voltage E causes a rotation of the mirror of G_1 by a signal current I_1. The photovoltaic cells then produce an amplified current I_2 measured by galvanometer G_2. This current I_2 also produces negative feedback in series with G_1. The negative feedback increases the stability, linearity and effective input impedance of the system.

As long as the current amplification $I_2/I_1 = M$ is fairly large, we may neglect I_1 and the applied voltage E is given by

$$E = I_2 R$$

where R is the feedback resistance. So, for a given signal E and feedback resistance R, the deflection of the secondary galvanometer G_2 depends only on its sensitivity and is relatively independent of the photocell amplification M as long as M is large.

It is interesting to calculate the effective

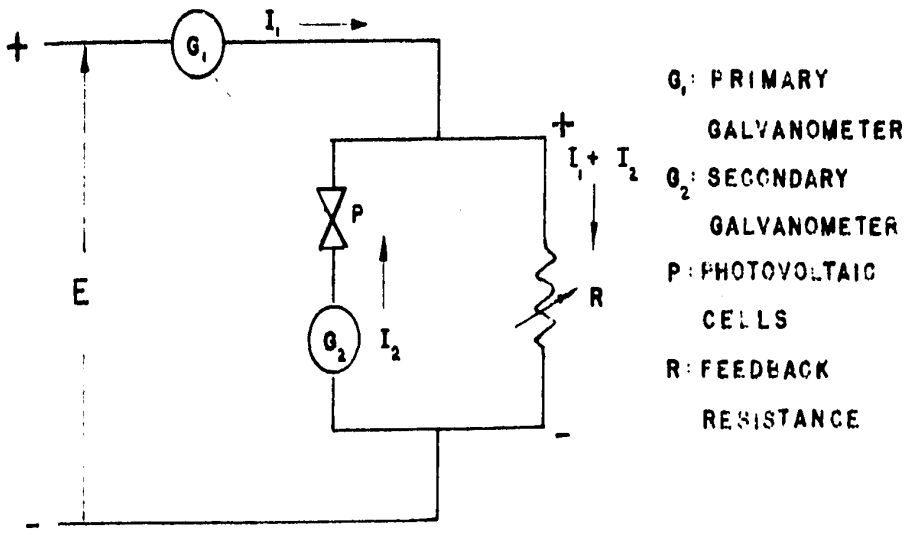

FIG. 8 - CIRCUIT OF THE GALVANOMER AMPLIFIER WITH AN APPLIED VOLTAGE OF ARBITRARY POLARITY.

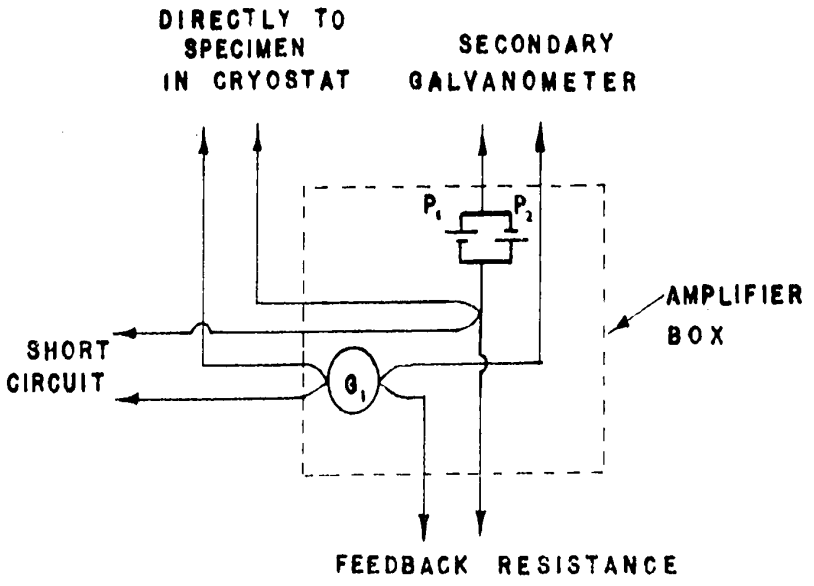

FIG. 9 - SIMPLE WIRING OF THE AMPLIFIER TO REDUCE VARYING CAPACITIES AND THERMAL NOISES AT HIGH SENSITIVITY.

input impedance R_e of this system. By definition,

$$R_e = \frac{E}{I_1}$$

However $E = I_2 R_1$ so

$$R_e = \frac{I_2 R}{I_1} = MR$$

The current amplification M is not a constant of the system but depends on the value of the feedback R. As R is increased, M decrease because of the larger resistance in the photocell circuit. M may be of the order of 200 with a feedback of 50 ohms. The effective input impedance MR is then 10,000 ohms. This resistance is very large compared to the specimen resistance of the order of 0.01 ohms. Therefore the galvanometer amplifier does not disturb appreciably the specimen current. Also the resistance of the voltage leads to the amplifier may vary with temperature without affecting appreciably the measurements.

The linearity of our galvanometer amplifier is demonstrated in figure 10 where the deflection of G_2 is plotted against a known applied voltage drop. Deviations from linearity are mainly caused by the secondary galvanometer itself.

Also, the sensitivity of the amplifier was found linearly proportional to the feedback resistance R, in

FEEDBACK RESISTANCE OF 1000 OHMS

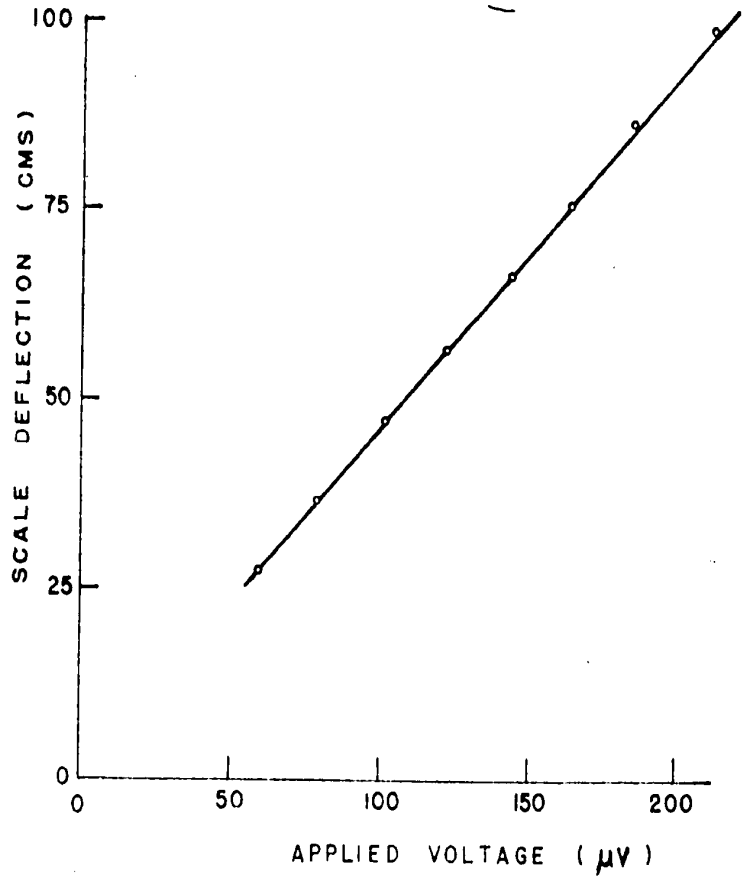

FIG 10 - LINEARLITY OF GALVANOMETER AMPLIFIER.

agreement with the theoretical performance equation $E = I_2R$.

2.6.3 Remarks on the Choice of Galvanometers for Amplifier

For measuring small voltages there is no objection to choosing a sensitive secondary galvanometer. We use a sensitive galvanometer with an internal resistance of 500 ohms. The scale is set at a distance of 3 meters from the galvanometer mirror.

For high sensitivity measurements however it is necessary to choose a primary galvanometer with a small internal resistance. This is because the primary galvanometer introduces noise which is amplified by the photovoltaic cells. A galvanometer introduces Brownian noise because of the fluctuations in the collisions of air molecules with the suspension and Johnson noise due to the fluctuations in the distribution of electrons in its resistance. It turns out that both these effects are of the same order of magnitude. They are really two different approaches to the same problem. (cf. Sear's Thermodynamics, 1953). The noise produced by the primary galvanometer must be a few orders of magnitude smaller than the signal to be measured. We use a primary galvanometer with 10 ohms internal resistance. It is quite satisfactory for measuring signals of the order of 1 microvolt.

2.6.4 Details of the Galvanometer Amplifier

Our galvanometer amplifier is quite conventional except that a rotating mirror is used to adjust the position of the beam of light on the photocells. This fine adjustment is done by turning a knob and without opening the box containing the photovoltaic cells and primary galvanometer. The optical system is drawn in figure 11 and a photograph is shown in figure 12.

The source of light is a 100 watt projector bulb. Its intensity is stabilized by means of a Sola transformer. The light is focussed on the mirror of the primary galvanometer G_1 by means of the plano-convex lens L_1. An infrared absorber F reduces the photovoltaic cell fatigue. The lens L_2 focusses the beam of light on the photovoltaic cells P_1 and P_2. Note that the photovoltaic cells have the opposite poles connected together as shown in figure 9.

2.6.5 Varying Capacities, Thermal Noise and Vibrations

In the first experiments, varying capacities were the main source of noise in the circuit of the galvanometer amplifier. Movements of the operator produced fluctuations of a few percent in a signal of about 1 microvolt. This has been reduced to a negligible level by simplifying the wiring as shown in figure 9. Also the voltage wires were shielded

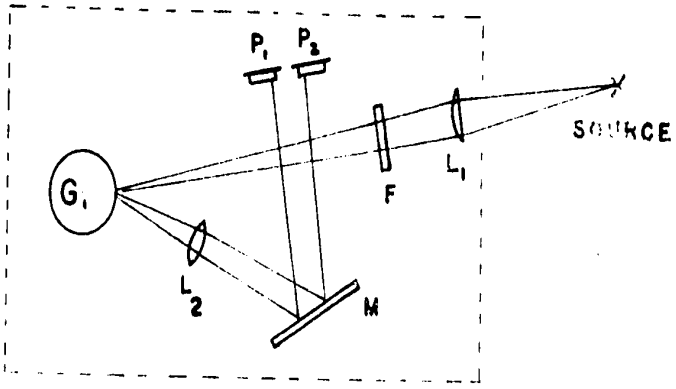

FIG. 11 - OPTICAL SYSTEM OF THE GALVANOMETER AMPLIFIER.

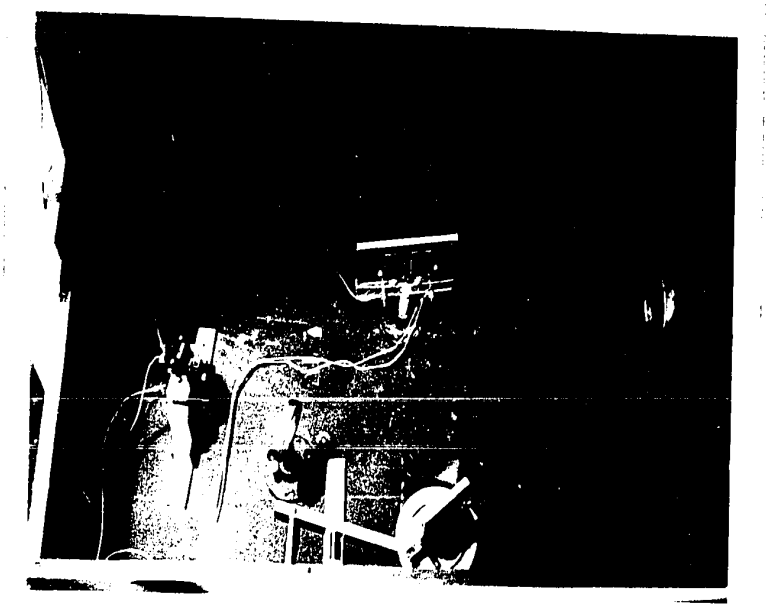

FIG. 12 - PHOTOGRAPH OF THE OPTICAL SYSTEM OF THE GALVANOMETER AMPLIFIER.

and the specimen grounded. This greatly reduced the varying capacity effects.

After these improvements thermal noise was important. There is a large thermal gradient along the wires bringing the signal out of the cryostat. This may be a very efficient source of thermal e.m.f.'s. As much as possible continuous copper wires free of kinks are used in the voltage circuit. Outside the cryostat these wires are connected by pressure contacts on thermally connected copper blocks. Also the feedback resistance box is filled with oil so as to reduce thermal fluctuations. Constant thermal e.m.f.'s do not affect our voltage measurements because we take the difference of readings with the current on and off.

Floor vibrations may also limit the sensitivity of the system. The amplifier box is sufficiently isolated from floor vibrations by placing it on a foam rubber pad and increasing its weight with heavy metal plates. Also the secondary galvanometer is placed on a cement block floating on a foam rubber pad.

2.6.6 Precision of Resistance Measurements

At liquid helium temperatures the voltages may be measured with a precision of about $\pm$ 0.1%. However sometimes during adiabatic demagnetizations the measurements are not so precise. This is probably due to thermal e.m.f.'s along

the voltage wires passing from the liquid helium bath to the specimen cooled by adiabatic demagnetization. In some experiments the voltages are still measured with a precision of about $\pm$ 0.2% below $1^{\circ}K$.

2.7 Measurement of Magnetoresistance

2.7.1 Method and Mounting

The resistance in a magnetic field is measured by the same method as the resistance in zero field. However the magnetoresistance measurements are taken only at $4.2^{\circ}K$ and about $1.1^{\circ}K$. So the specimens are placed directly in the liquid helium bath and the magnetic field is applied perpendicularly to them. Shorter specimens and larger currents may be used than in resistance measurements below $1^{\circ}K$. A section of the specimen support is shown in Figure 14. Separate current and voltage contacts are pressed against each end of the specimen. The pressure contacts avoid the effects observed with superconducting solder contacts placed in a magnetic field.

2.7.2 Electromagnet

A small Weiss type electromagnet mounted on tracks, is used both for magnetic cooling and magnetoresistance measurements. It can be used for long periods with a maximum current of 4.5 amperes which gives a field of about 5.2 kOe

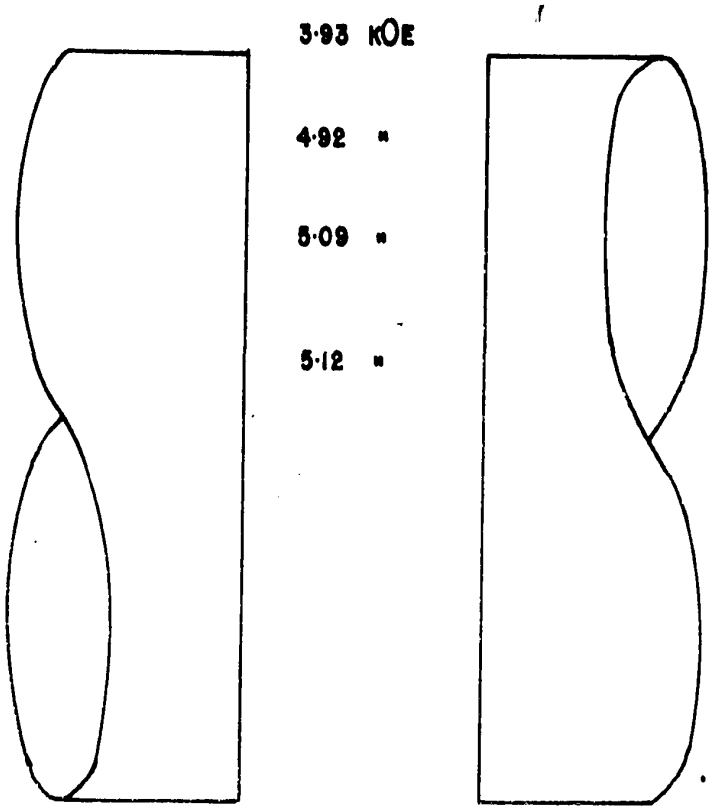

FIG. 13 - VARIATION OF H ACROSS THE POLE FACES FOR A 3·0 A MAGNET CURRENT AND 1·59" GAP.

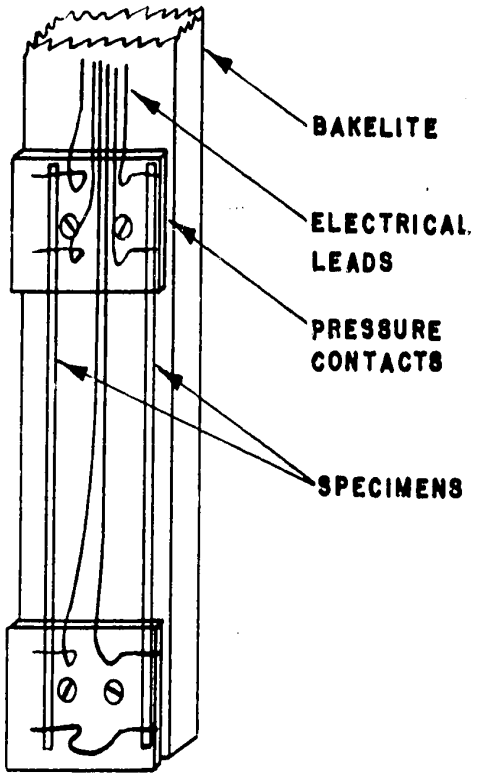

FIG. 14 - MOUNTING OF SPECIMENS FOR MAGNETORESISTANCE.

with a pole gap of 2.12 inches. The magnet current is stabilised over long periods by a control system which samples the current and regulates the exciter current of the generator*. The field of the magnet is calibrated against its current. The field is measured by a Rawson flux meter to ± 0.2% but the magnet current is known only to ± 1%. An hysteresis of the orders of 50 oersteds could be detected on decreasing the field. The magnetic field is fairly constant over a large fraction of the magnet gap. Figure 14 shows approximately the decrease in intensity from the center of the pole faces to the edge. For magneto-resistance measurements the specimen is placed near the center of the poles in a region where the field varies only by about 1%.

For magnetic cooling, the paramagnetic salt is placed near the center of the poles. If there is a small field gradient in the salt, the copper wires quickly establish thermal equilibrium after demagnetizing.

2.5 Precision of Measurements

The precision of measurements has been discussed throughout this chapter. For convenience a resume of these discussions is now given.

---

* Thanks to Dr. Hedgcock for providing this current control system.

The resistance measurements are usually precise to about $\pm$ 0.1%. Below 1°K the scatter in the measurements may increase to $\pm$ 0.2%. At five or six temperatures from 4.2°K to 1.3°K, four measurements of resistance and temperature are rapidly taken in succession. During these measurements the temperature of the helium bath often decreases by 0.1°K. Each temperature is measured to $\pm$ 0.01°K but an average is taken of each group of four readings and plotted as a single point on the resistance versus temperature diagram. A continuous curve is passed through these points.

Below 1°K the resistance and temperature measurements are slightly less precise. The main error in the temperature is due to the fact that the Δ -correction is neglected and that the uncorrected magnetic temperature cannot be converted into absolute temperatures. These errors are of the order of $\pm$ 0.05°K. Near 0.2°K the error may be slightly larger due to a lack of thermal equilibrium between the paramagnetic salt and the specimen. However all these errors do not affect the main conclusions drawn from the resistance measurements.

Usually the resistance in a magnetic field may be measured with the same precision as in the absence of a magnetic field. However the magnetoresistance is defined

as $(R_H - R_{H=0})/R_{H=0}$. This is often multiplied by 100 and expressed as a percentage. Since magnetoresistance involves a difference of resistance measurements, the precision of magnetoresistance measurements depends greatly on their magnitude. When the magnetoresistance is small, the errors in the resistance are important and the precision is low. For example the magnetoresistance may be the 0.3% with an accuracy of $\pm$ 25% (of the 0.3%). When the magnetoresistance is larger the error in the field intensity becomes important. For example the magnetoresistance may be of 25% with an accuracy of $\pm$ 1% (of the 25%) due to the error in the magnetic field.

In a few instances the current regulators did not control properly and there were low frequency fluctuations in the magnet current. Apparently this caused fluctuations in the field intensity and induced noise in the measured voltage drop. For this reason the scatter in the magnetoresistance readings is sometimes slightly larger than usual.

2.3 Preparation of Mg (Mn) Specimens

The specimens were prepared from magnesium ingots with a nominal content of 0.44 and 0.66 atomic percent manganese. Ribbon like specimens about 0.15 mm thick and 30 mm long were obtained by rolling at temperatures above

200°C. After rolling and etching, the specimens were annealed and sometimes quenched at high temperatures in order to keep as much Mn as possible in solid solution. The specimen tube for heat treatments was usually filled with half an atmosphere of argon before annealing. Sometimes also, carbon was added in the specimen tube to decrease the oxidation of the specimen. The particular heat treatment of each of seven specimens is given in table 2. The measured resistance ratio $R_{4.2}/R_{273}$ is also given in this table. It is seen that the specimens quenched at high temperatures usually have the largest resistance ratio indicating that there is more Mn in solid solution. Besides a few resistance and magnetoresistance curves, the measurements taken on these seven specimens are summarized in table 3, Chapter XI.

The concentration of Mn in these alloys is not known accurately. For the very dilute alloys the amount of Mn in solid solution is approximately proportional to the measured resistance ratio $R_{4.2}/R_{273}$. More precisely, if the alloy obeys Nordheim's and Matthiessen's rule and if the thermal expansion is negligible, then the concentration of solute in solid solution is linearly proportional to $(R_{4.2}/R_{273} - R_{4.2})$. However dilute Mg (Mn) alloys do not follow these laws closely; $R_{4.2}$ is anomalous.

In collaboration with other research workers we have tried to estimate roughly the relation between the atomic

Table 2

Preparation of Specimens

Specimen	Sample source	Sample Treatment	$\frac{R_{4.2}}{R_{273}}$
1	Dow Chemical Co. Nominally 0.45 at. % Mn.	Annealed 20 hours at 450°C argon atm., cooled slowly	0.152
2	Same as for specimen 1	Annealed 20 hours at 450°C argon, cooled slowly.	0.212
3	Dow Chemical Co. Nominally 0.65 at. % Mn	Annealed 3 hours at 490°C argon and carbon present quenched in ice water	0.305
4	Same as for specimen 3	Annealed 22 hours at 525°C argon and carbon present quenched in ice water	0.532
5	Dow Chemical Co. Nominally 0.45 at. % Mn	Annealed 20 hours at 450°C cooled slowly	0.073
6	Same as for specimen 1	Annealed 20 hours at 450°C argon atm., cooled slowly	0.170
7	Same as for specimen 3	Annealed 22 hours at 525°C argon and carbon quenched in ice water	0.335

percent of Mn in Mg and the ratio $R_{4.2}/(R_{273} - R_{4.2})$. As a first approximation we assume that this relation is linear as for ideal dilute alloys. Also we assume that the specimen with the largest resistance ratio did contain the maximum amount of Mn that can be dissolved in Mg. The maximum solubility is given by the phase diagram of the system (Metals Handbook, 1948). The broken line of figure 15 shows the estimated atomic % of Mn in Mg as a function of the ratio $R_{4.2}/(R_{273} - R_{4.2})$. This atomic % concentration may be in error by as much as ± 20%. The point plotted near the origin of figure 15 corresponds to a set of values quoted by Spohr and Webber (1956).

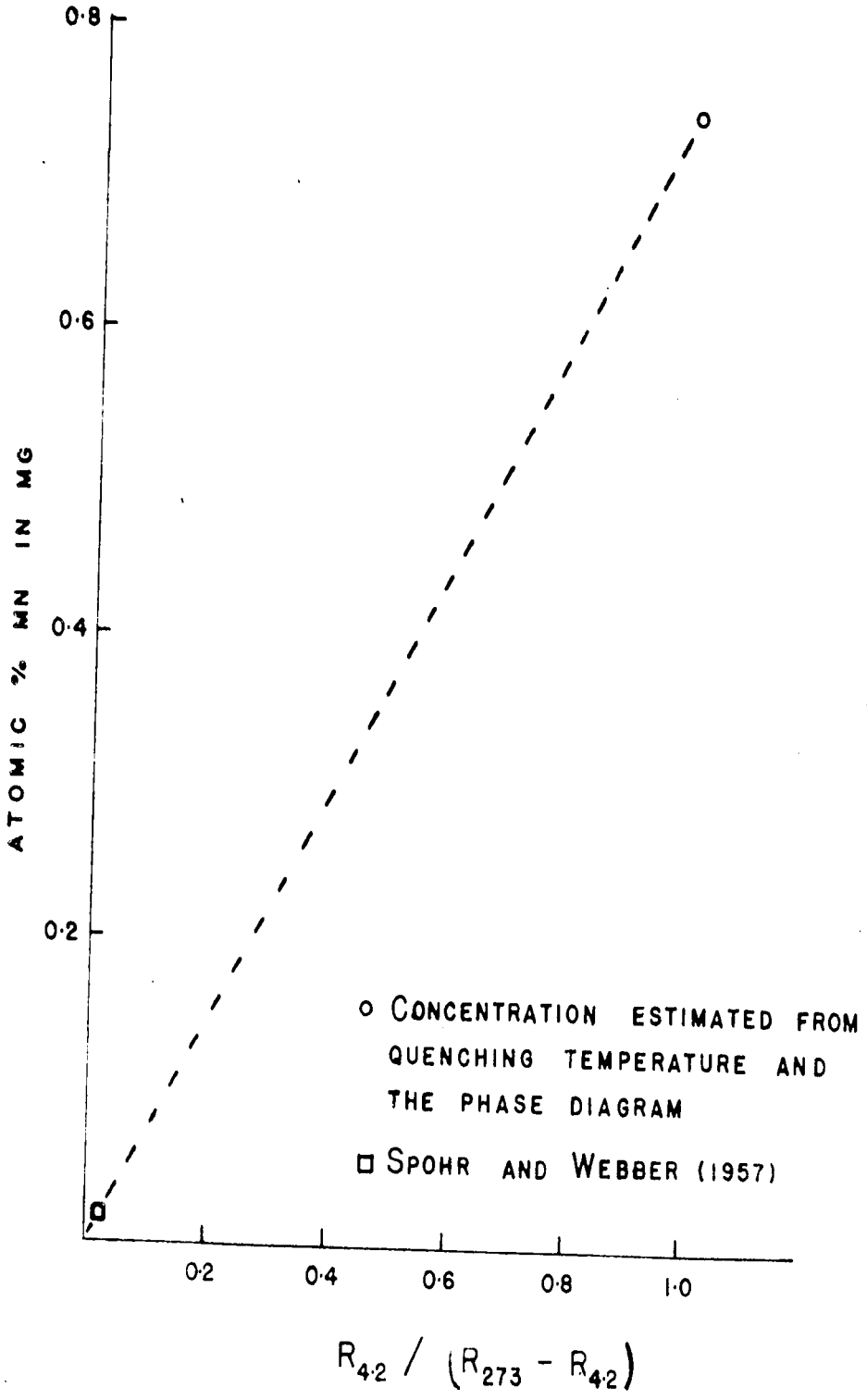

FIGURE 18 – ROUGH ESTIMATE OF THE ATOMIC % MN IN MG VERSUS THE NORMALIZED RESISTANCE RATIO $R_{4\cdot2} / R_{273} - R_{4\cdot2}$.

CHAPTER 3

3.1 Previous Measurements on Mg (Mn) Alloys

The resistance minimum of Mg (Mn) alloys was first reported by Meissner and Voigt (1930) and later by Keesom (1933). In recent years many workers have observed this minimum such as MacDonald and Mendelssohn (1950), Garfunkel, Dunnington and Serin (1950), Rorschach and Herlin (1951), Yntema (1953) and Rosenberg (1954). In all these measurements a resistance minimum was observed at temperatures of the order of 10^{0} K and the resistance increased monotonically down to the lowest temperatures.

The measurements of Yntema (1953) were particularly on the magnetoresistance at temperatures below the temperature of the resistance minimum. His specimen had a resistance ratio $R_{4.2}/R_{273} \approx 5 \times 10^{-3}$ and the zero field resistance increased by about 4% from 4.2^{0} K to 1.3^{0} K. The variation of magnetoresistance from 4.2^{0} K to 1.3^{0} K was in agreement with Kohler's rule and the significance of this fact was thoroughly discussed by Yntema.

Recently many experiments were performed on the same specimen of Mg (Mn) at the U.S. Naval Research Laboratory. Careful attention was given to the possibility of a resistance maximum in these alloys. Spohr and Webber (1956) have

observed that this specimen had a resistance ratio $R_{min}/R_{300} = 24.4 \times 10^{-3}$ and a resistance minimum at 14.5° K. Hein and Falge (1956) have further observed that the resistance of this specimen increased monotonically down to 0.2° K. The resistance increased by 24% from 4.2° K to 0.22° K. Also Webber (1956) has measured the magnetoresistance of this specimen at 4.2° K and 1.3° K. The variation of magnetoresistance from 4.2° K to 1.3° K deviated by about 10% from Kohler's rule. By following Gerritsen's classification (1953) these results were taken to suggest a possible resistance maximum in Mg (Mn) alloys. However, as explained in the first chapter, the Gerritsen classification is not generally valid and deviations from Kohler's rule are not sufficient to imply a resistance maximum.

More recently, Hedgcock, Muir and Wallingford (1960) have made extensive measurements on the resistance minimum of Mg (Mn) alloys. The temperature of the minimum varied from 6° K to about 15° K.

Dilute magnetic alloys with monovalent parent metals sometimes also have a resistance maximum below the minimum. However such a resistance maximum has never been observed in a dilute magnetic alloy with a divalent parent metal such as Mg. Therefore it was very interesting to look for

a maximum in the resistance of Mg (Mn) alloys. We have done this by taking resistance measurements on more concentrated Mg (Mn) alloys down to very low temperatures.

3.2 Results of Resistance and Magnetoresistance Measurements on Mg (Mn) Alloys

The electrical resistance and magnetoresistance measurements taken on seven specimens of Mg (Mn) are summarized in Table 3. The resistance curves of four specimens are given in Figures 16 and 17. In these figures, the electrical resistance relative to the resistance at 273° K is plotted versus the temperature. This is the absolute temperature above 1.3° K and the uncorrected magnetic temperature T* below 1.3° K (see section 2.5.3). Each plotted point corresponds to an average of four resistance and four temperature measurements.

It is evident from these graphs that Mg (Mn) alloys have a resistance maximum at temperatures below the resistance minimum. In some cases the resistance decreases by more than 5% at temperatures below the maximum. At temperatures below 4.2° K, the resistivity due to thermal vibrations is negligible. Therefore these curves in effect represent the behavior of the impurity resistivity.

Table 1

Tabulation of Resistance and Magnetoresistance Measurements on a Few Mg (Mn) Alloys

Specimen	Resistance $\frac{R_{4.2}}{R_{273}}$	Resistance T_{max}	Resistance $\frac{R_{1.3}}{R_{4.2}}$	Magnetoresistance ΔR_H
1	0.152	1.2	1.04	
2	0.212	1.8	1.01	$\Delta R_H > 0$ at 4.2° K $\Delta R_H < 0$ at 1.28° K
3	0.305	2.8	0.99	
4	0.532	>4.2	0.97	
5	0.073	<1	1.09	$\Delta R_H > 0$ at 4.2° K and 1.21° K. Large deviation from Kohler's rule.
6	0.170	≈ 1.3	1.03	$\Delta R_H > 0$ at 4.2° K $\Delta R_H = 0$ at 1.31° K
7	0.335	3.3	0.99	$\Delta R_H > 0$ at 4.2° K $\Delta R_H < 0$ at 1.28° K

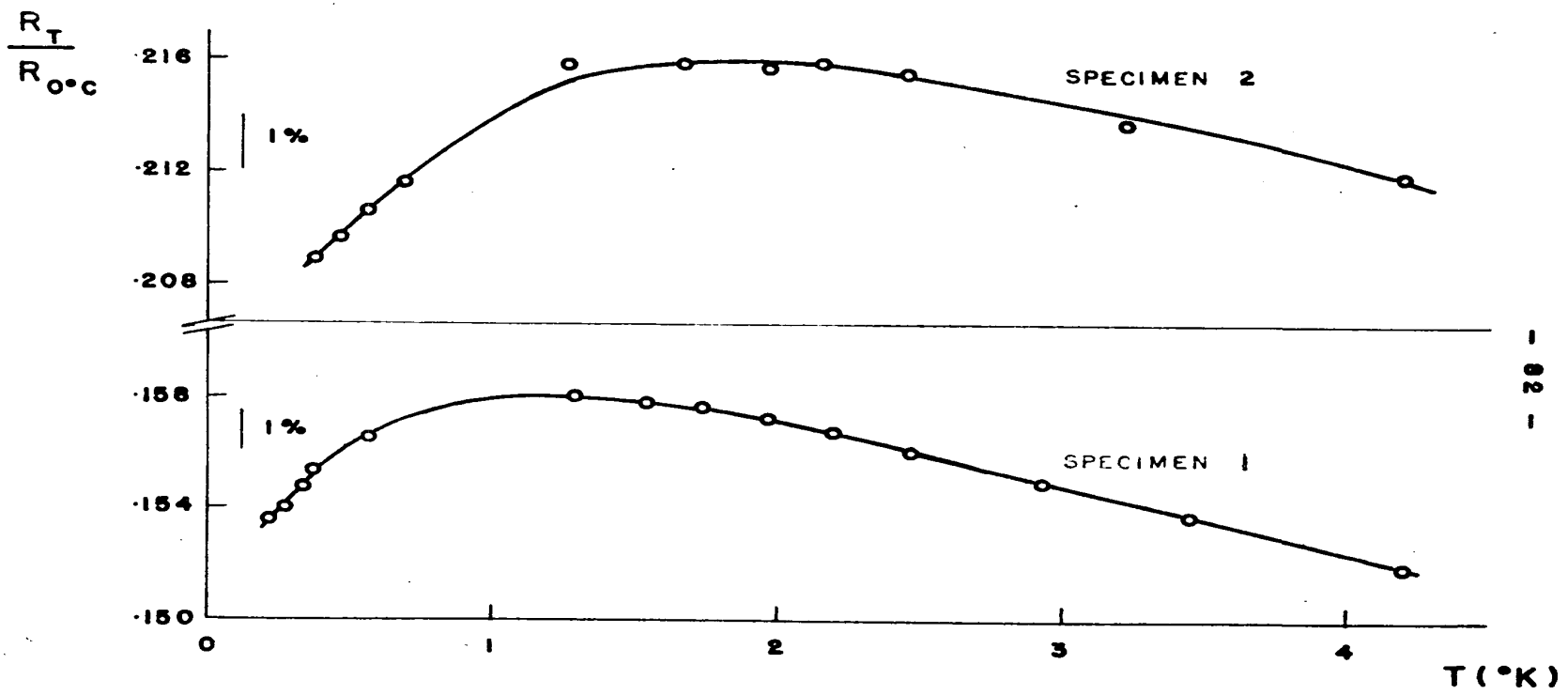

FIG. 16 – RELATIVE ELECTRICAL RESISTANCE VERSUS TEMPERATURE OF TWO DILUTE MG(MN) ALLOYS.

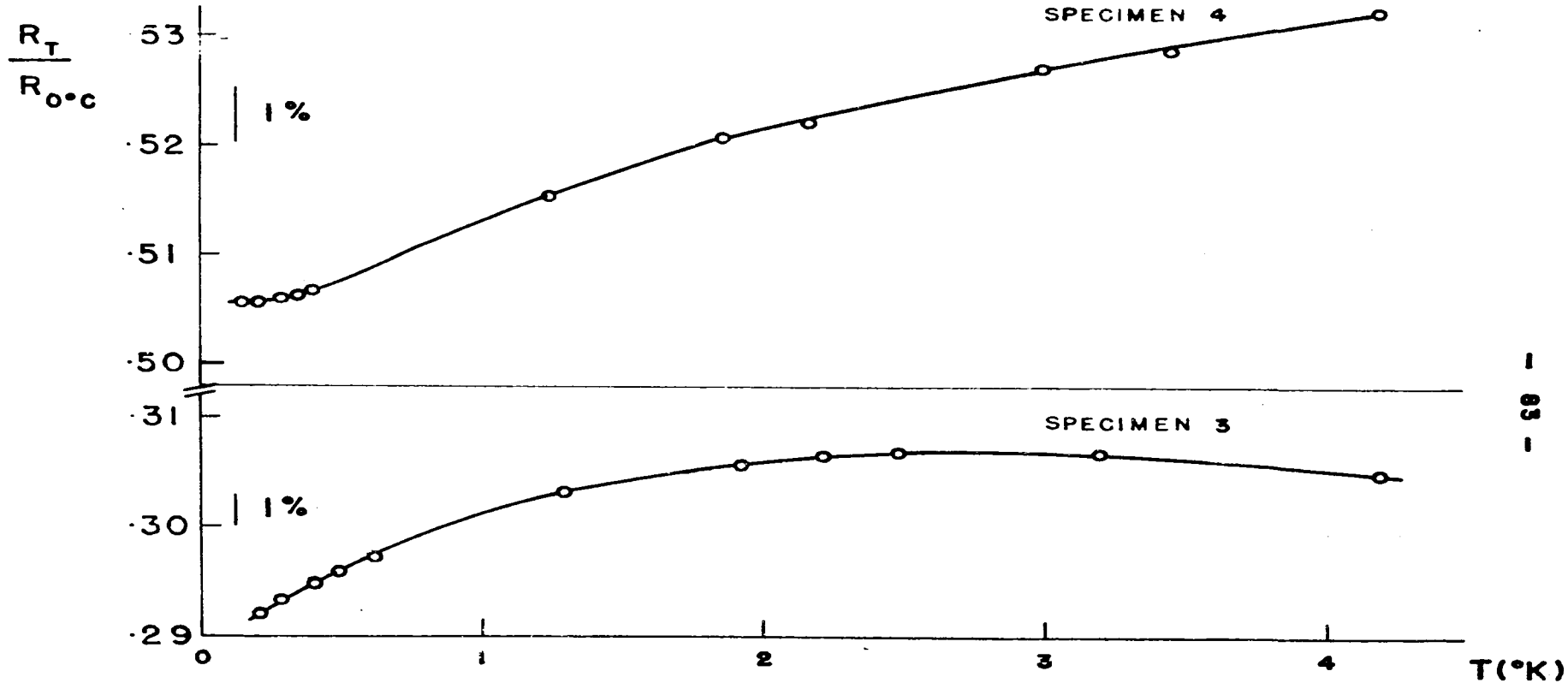

FIG. 17 – RELATIVE ELECTRICAL RESISTANCE VERSUS TEMPERATURE OF TWO MOST CONCENTRATED MG(MN) SOLID SOLUTIONS.

The resistance maximum of specimen 4 is not seen in Figure 17 because it occurs above 4.2° K. The resistance of this specimen was measured down to 0.16° K and it appears to become nearly constant near 0.2° K. However this small effect remains dubious because of the following reasons; The warm up time after the adiabatic demagnetization was shorter than usual; therefore the specimen had less time to reach thermal equilibrium with the salt. Also the thermal link between the specimen and the salt was not as reliable as usual. In the other experiments, the resistance specimens were fairly long (~ 25 cms). These long specimen could be wound all along the specimen support and be in good thermal contact with it. However specimen 4 was partially destroyed when annealed at high temperatures and the short piece left was mounted near the pressure contacts. Near the contacts. he thermal link with the salt is not as good as elsewhere. Therefore further experiments will be necessary to verify whether the resistance of Ag (Mn) becomes constant at very low temperatures below the maximum.

It is evident from the resitance curves that T_{max} increases with the ratio $R_{4.2}/R_{273}$. We can determine T_{max} to about ± 0.3° K. It is shown by Figure 18 that within the accuracy of measurements, T_{max} is linearly proportional to $R_{4.2}/(R_{273} - R_{4.2})$. However we do not know exactly the concentration of Mn that corresponds to a measured resistance

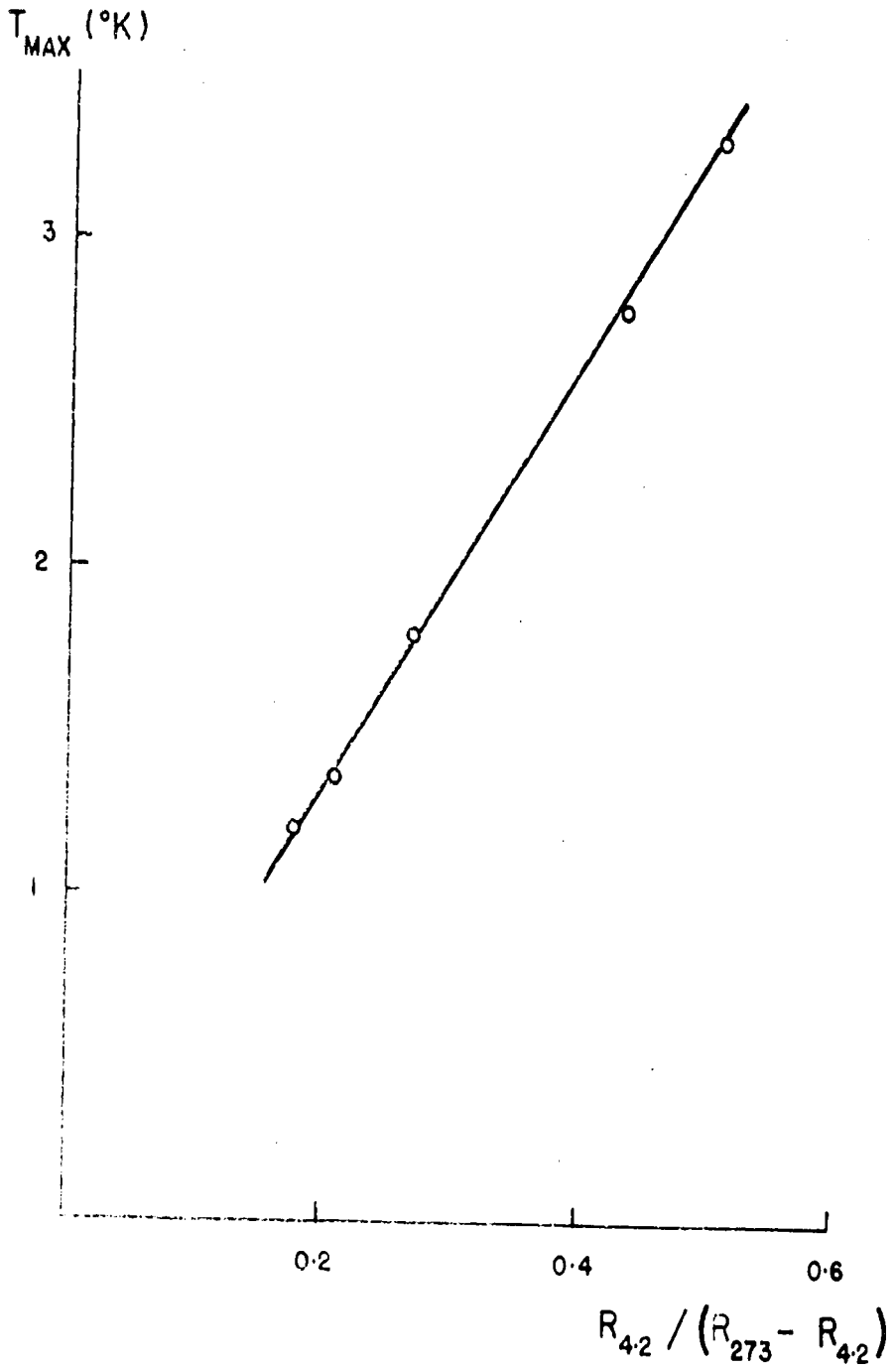

FIGURE 18 - TEMPERATURE OF THE RESISTANCE MAXIMUM OF MG(MN) ALLOYS VERSUS $R_{4·2} / (R_{273} - R_{4·2})$ THIS RATIO IS APPROXIMATELY PROPORTIONAL TO THE CONCENTRATION OF MANGANESE.

ratio (see section 2.4 and the rough estimate plotted in Figure 15). Therefore T_{max} increases with the concentration of Mn dissolved in Mg but it is not certain that this relation is linear.

Besides these electrical resistance measurements, the magnetoresistance of a few Mg (Mn) alloys has been measured at 4.2° K and near 1.3° K in magnetic fields up to about 5.5 kOe.

In Figure 19 (A), the magnetoresistance of specimen 5 is plotted directly versus the magnetic field intensity. It is seen that the magnetoresistance at 1.21°K is much smaller than at 4.2° K although there is only a small increase in the zero field resistance. This behavior does not appear to follow Kohler's rule. In order to verify this, a Kohler plot is made of these measurements in Figure 19 (B). The measurements taken at the two temperatures do not fall on the same curve, as they should if Kohler's rule was obeyed. It is interesting to observe that specimen 5 contains about three times more Mn than the Webber specimen (Webber, 1956) and the deviations from Kohler's rule are of about 40% instead of 10%.

The magnetoresistance of specimens 6 and 7 is plotted in Figure 20. For these two specimens, the deviations from Kohler's rule are so obvious that Kohler plots are not necessary. The magnetoresistance of specimen 6 decreases

SPECIMEN 5

(A)

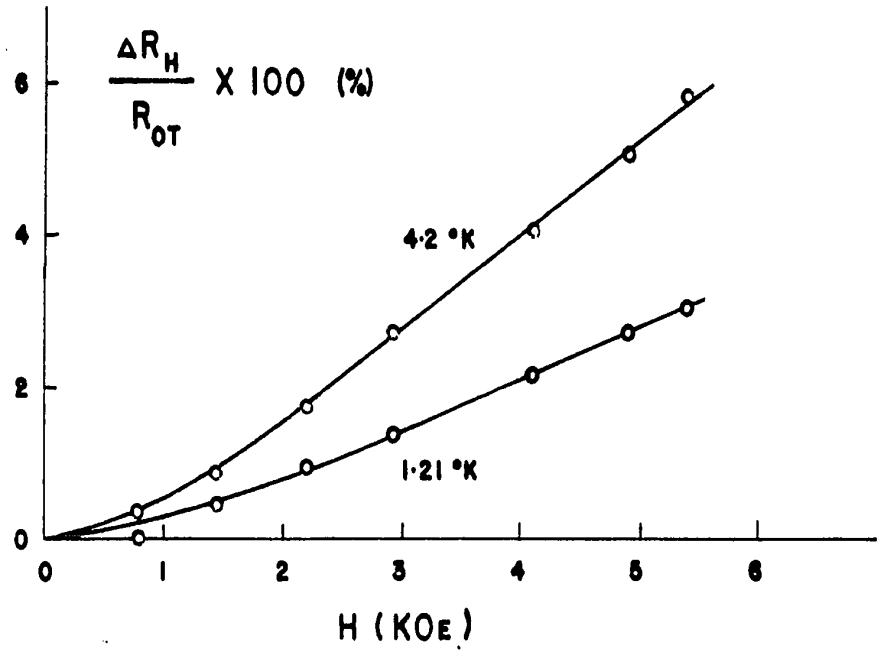

(B)

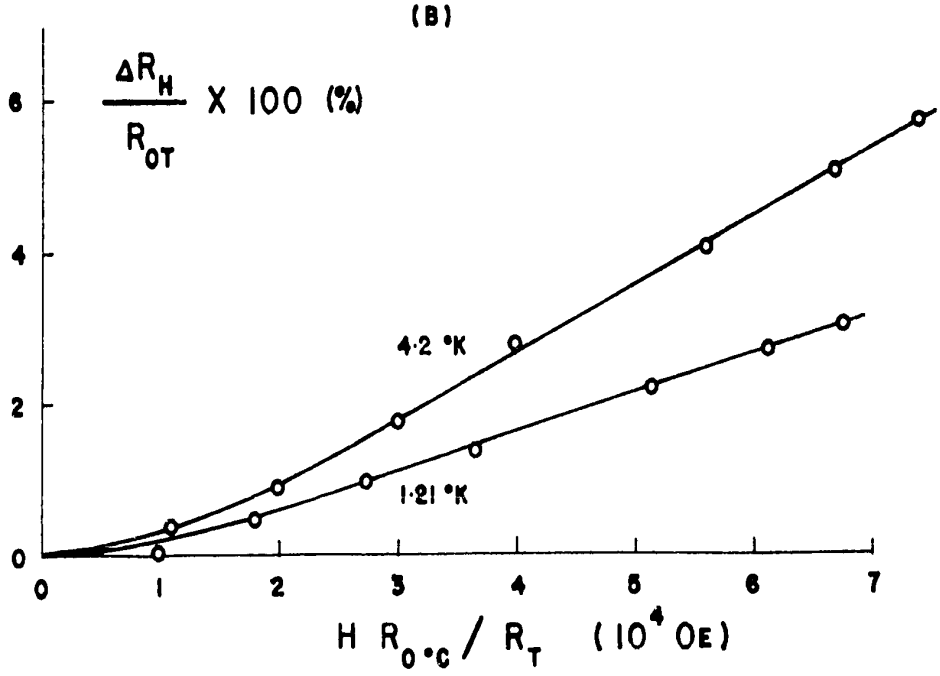

FIG. 19 – MAGNETORESISTANCE OF A DILUTE Mg(Mn) ALLOY (A) PLOTTED VERSUS MAGNETIC FIELD INTENSITY AND (B) KOHLER PLOT. THIS SPECIMEN HAD NO MAXIMUM ABOVE 1°K. $R_{4.2\,°K} / R_{0\,°C} = 0.073$.

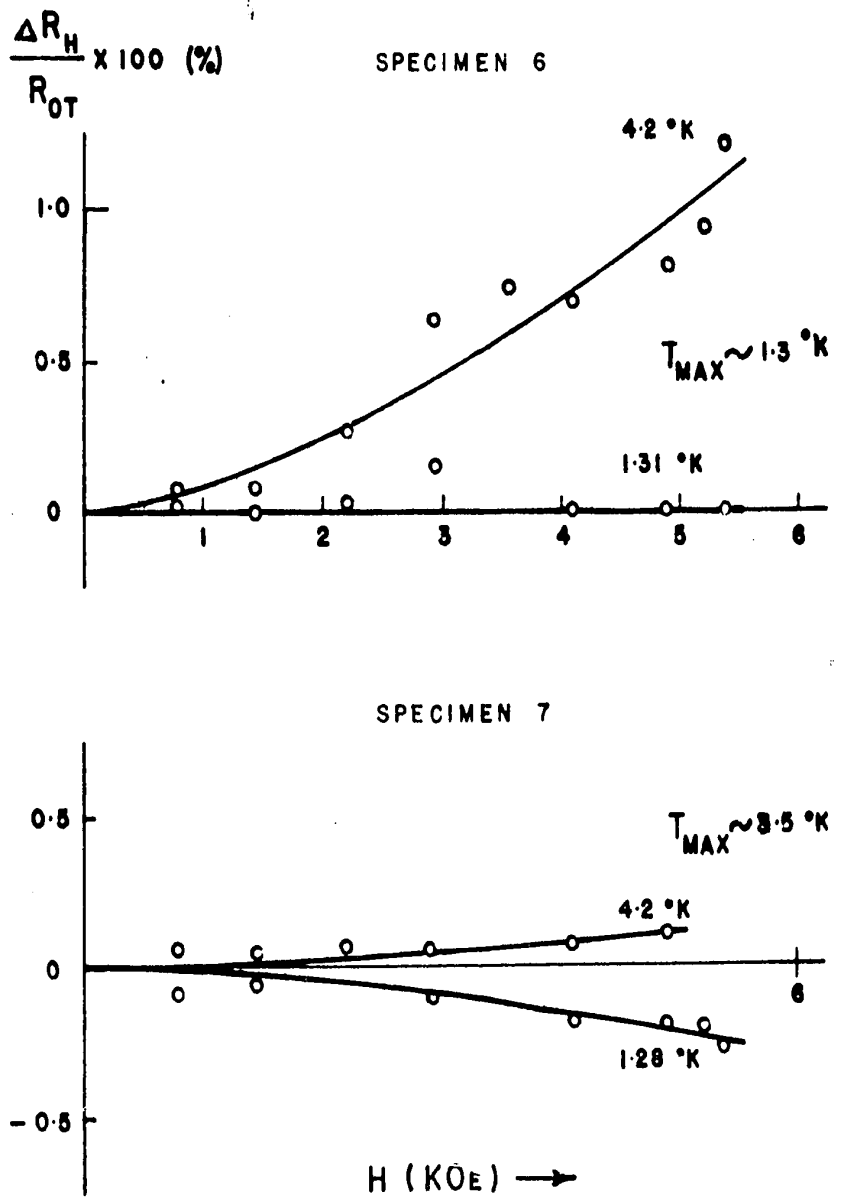

FIG. 20 - MAGNETORESISTANCE OF TWO SPECIMENS OF Mg(Mn) AT TEMPERATURES NEAR THE RESISTANCE MAXIMUM. $R_{4.2\,°K} / R_{0\,°C}$ EQUALS 0·170 FOR THE UPPER GRAPH AND 0·335 FOR THE LOWER ONE.

rapidly with temperature. It is positive at 4.2° K and zero at 1.31° K. The magnetoresistance of the more concentrated specimen 7 is also positive at 4.2° K but it even becomes negative at 1.28° K.

The magnetoresistance of specimen 7 is definitely negative at 1.28° K; however this decrease is of less than 0.3% at the highest fields available. It would be interesting to measure precisely the relation between $\Delta R/R$ and H at higher fields to verify if this negative magnetoresistance changes with the square of the field intensity (or more precisely the square of the magnetization) as for some other dilute magnetic alloys.

3.3 Conclusions

It is now apparent that the resistance maximum of Mg(Mn) alloys was not previously observed because the specimens did not contain enough Mn in solid solution; measurements at much lower temperatures might also have shown a resistance maximum.

It is yet too early to make detailed qualitative comparisons between these experimental results and the theories. The problem is very complex since it involves randomly distributed ions in the lattice and many possible types of ion-ion interactions and electron-ion interactions.

We can conclude from these measurements that as it was previously observed with many monovalent parent metals,

(1) Mn impurities causes a resistance maximum in divalent Mg,

(2) the temperature of the maximum increases rapidly with the concentration of Mn and

(3) the magnetoresistance decreases rapidly at temperatures below the minimum and even becomes negative around the temperature of the resistance maximum.

These results suggest that the valency and the crystal structure of the parent metal are not extremely important factors in the occurrence of a resistance maximum. These measurements do not provide extremely new evidence on the origin of the resistance maximum but they do lend support to the belief that such anomalies are related to the magnetic and exchange properties of transition element impurities.

BIBLIOGRAPHY

Brickwedde, Physica, 24, S128 (1958).

Brailsford, A.D. and A.W. Overhauser, Phys. Rev. Letters, 3, 331 (1959).

Coles, B.R., Phil. Mag. Supplement, 7, 40 (1958).

Croft, Faulkner, Hatton, Seymour, Phil. Mag, 44, 289 (1957).

de Gennes, P. and Friedel, J., J. Phys. Chem. Solids, 4, 71 (1958).

de Haas, de Boer and van den Berg, Physica, 1, 1115 (1933).

Dekker, A.J., Physica, 24, 697 (1958).

Dekker, A.J., Physica, 25, 1244 (1959).

Dekker, A.J., Solid State Physics, London (1958).

Friedel, J., J. Phys. Rod., 19, 573 (1958).

Garfunkel, Dunnington and Serin, Phys. Rev., 79, 211 (1950).

Gaudet, G., Hedgcock, F.T., Lamarche, G. and Wallingford, R.W., Can. J. Phys., 38, 1134 (1960).

Gerritsen, A.N. and Linde, J.O., Physica, 17, 573 (1951).

Gerritsen, A.N., Physica, 19, 61 (1953).

Gerritsen, A.N., Physica, 25, 498 (1959).

Hein, R.A. and Falge, R.L., Phys. Rev., 105, 1433 (1957).

Jacobs, I.S. and Schmitt, R.W., Phys. Rev., 113, 459 (1959).

Korringa, J. and Gerritsen, A.N., Physica, 19, 457 (1953).

Linde, J.O., Physica, 24, S109 (1958).

MacDonald, D.K.C., Encyclopedia of Physics, Springer, Berlin vol. 14, 137 (1956).

MacDonald, D.K.C. and Mendelssohn, K., Proc. Roy. Soc. A, 202, 523 (1950).

MacDonald, D.K.C. and Sarginson, K., Rep. Progr. Phys., 15, 249 (1952).

Mott, N.F. and Jones, H., Metals and Alloys, New York (1958).

Pearson, W.B., Phil. Mag., 46, 911 (1955).

Pearson, Rimek and Templeton, Phil. Mag., 4, 612 (1959).

Pearson, W.B., Phil. Mag., 4, 622 (1959).

Pratt, G.W., Phys. Rev., 106, 53 (1957).

Rorschach, H.E. and Merlin, M.A., Phys. Rev., 81, 467 (1951).

Rosenberg, H.M., Phil. Mag., 45, 73 (1954).

Sato, Arrott and Kikuchi, Phys. Chem. Solids, 10, 19 (1959).

Schmitt, R.W., Phys. Rev., 103, 83 (1956).

Schmitt, R.W. and Jacobs, I.S., Can. J. Phys., 34, 1285 (1956).

Sears, F.W., An Introduction to Thermodynamics, etc., Addison-Wesley (1953).

Spohr, D.A. and Webber, R.T., Phys. Rev., 105, 1427 (1957).

Strong, J., Modern Physical Laboratory Practice, London (1950).

Thomas, J.G. and Mendoza, E., Phil. Mag., 43, 900 (1952).

Webber, R.T., Phys. Rev., 105, 1437 (1957).

White, G.K., Experimental Techniques in Low Temperature Physics, Oxford Press (1959).

Wilson, A.H., The Theory of Metals, Cambridge University Press, 2nd edition, 1953.

Yntema, G.B., Phys. Rev., 91, 1388 (1952).

Yosida, K., Phys. Rev., 106, 893 (1957).

Zener, C., Phys. Rev., 81, 440 (1951).

Zener, C. and Heikes, R.R., Revs. Modern Phys., 25, 191 (1953).

Ziman, J.M., Electrons and Phonons, Oxford Press (1960).

VITA

Name: Gilles Gaudet

Born: Laverlochere, Prov. of Quebec, 1935

Educated:

Primary	Laverlochere, 1941-47
Secondary	Ottawa University High School, 1947-51
University	Ottawa University, 1951-57
Course	Physics
Degree	B.Sc. (honours) 1957